MSUCP-44

July 1985

COMPUTATIONAL STUDY OF THE MARK IV EXTRACTION SYSTEM FOR THE K800 CYCLOTRON

D. Johnson, V. Taivassalo, M. Gordon and H. Blosser

I. Introduction

Extracting the beam from the K800 cyclotron is a difficult problem. There is first of all the basic difficulty of all high field cyclotrons, namely that the magnetic field is approximately three times stronger than in normal cyclotrons whereas techniques for making a comparable increase in the strength of electric fields are not available. Since cyclotron extraction systems depend on using an electric field to offset a given fraction of the magnet field, extracting the beam becomes more difficult as the magnetic field is increased. Typical high field extraction systems then make extensive use of "magnetic channels" either passive or active or both as the major strong orbit straightening force; unfortunately, the field of such magnetic elements is usually not well localized and the design must then account for, and compensate for, the effects of these "fringe" fields on the beam in orbits preceeding the extraction turn.

In addition to the "normal" high field problem described above, several aspects of the K800 cyclotron act to make extraction particularly difficult. These include:

a) If one takes the extraction system of the K500 as a design starting point and applies scaling rules, one would expect the maximum electric field to increase in proportion to the maximum projectile velocity (since for given geometry the electric field must offset a given fraction of the v x B force). The maximum design velocity for the K800 is 46% higher than the design maximum for the K500, and one therefore requires either higher electric fields or a "tighter" design. The situation is further exacerbated by the fact that experience with the K500 indicates that electric fields assumed in that design are quite difficult to achieve in practice, and an extraction system with electric fields reduced relative to the design values for the K500 is what is really wanted for the K800.

b) The high specific energy (200 MeV/nucleon) of the K800 means that the operating point is very near the "three-halves stop band", a radial focusing oscillation resonance which marks the ultimate stability limit for a 3-sector cyclotron. This resonance plus the essential coupling resonance $\nu_r+2\nu_z=3$ give unusually demanding requirements on the level of imperfections which can be tolerated in the magnetic field in order to hold the beam accurately on center as it passes these and the usual imperfection and coupling resonances ($\nu_r=1$ & $\nu_r=2\nu_z$) which occur near the edge of the

cyclotron. The very tight pole tip spiral is also an important factor contributing to tolerance sensitivity.

c) The magnet gap in the K800 cyclotron is 20% larger than the gap in the K500 (3" vs 2.5"). This has important advantages in easing a number of mechanical problems including problems associated with the deflector design, but further adds to the burden on the extraction system by reducing the sharpness of the "fall-off" of the magnetic field at the edge of the magnet. (The fundamental role of the electric field in the extraction system is to increase the radius of curvature such that the final internal orbit effectively extends beyond the fixed point associated with $\nu_r = 0$ -- the "softer" field edge given by the larger magnet gap moves this fixed point out in radius -- a larger fractional change in radius is therefore required to push the orbit into the "break-free" region.)

Studies of possible extraction systems for the K800 are largely undocumented except for the earliest studies. Noting this, we then first briefly review the various major thrusts and conclusions from the earlier studies before proceeding with presentation of results for the specific system which is the subject of this report.

II. Review of Prior Extraction System Studies

A first solution to the K800 extraction problem, which we label here the Mark I extraction system, was described in the Conceptual Design Report

(MSUCL-282, December 1978). This extraction system assumed electric fields of 140 kV/cm, the same design maximum value as assumed in the design of the K500 extraction system. The design procedure also assumed that the magnetic fringing fields from the extraction elements have negligible effect on the internal beam, provided that compensating elements which were included in the design are adjusted appropriately, this being an assumption which had worked adequately in the design of the K500 extraction system. Within the framework of these assumptions, a design for an extraction system was developed. The system involved two electrostatic deflectors, six moveable sets of magnetic "focusing bars", and three magnetic "compensating bars". The system closely paralleled the K500 extraction system except that one of the magnetic elements preceded the second electrostatic deflector in order to provide additional bending effect and improved focusing characteristics. (This location unfortunately places the focusing bar considerably closer to the internal beam region of the cyclotron than any of the K500 bars.)

Following the Conceptual Design Report, a period of years passed in which little was done on the K800 extraction system -- the system as described in the report was thought to be a good one -- the staff was heavily involved in the starting up of the K500 -- and the group from Milan, who had primarily performed the studies described in the Conceptual Design Report, had returned to their home Laboratory thereby leaving a major void in the accelerator computing staff at NSCL. When extraction studies for the K800 later resumed, computer results soon showed an important deficiency in the previous studies, namely that internal beam perturbations due to the fringing fields of the magnetic extraction elements were large, even dominant, in the situation of the K800. The assumption that these effects could be made negligible by adjustment of the compensating elements was

quite incorrect, at least for the specific system of compensating elements envisioned in the Mark I design.

One can of course always assert a solution in principle to the compensation problem by simply requiring that all magnetic elements be replicated in every sector. This is however not mechanically feasible, or at least extremely difficult, in the constrained and intricate geometry of the K800. Therefore, after many weeks of computer searching produced only one example of a viably extracted beam, a decision was made to shift attention to other possible extraction geometries.

Concurrently with the above studies of the compensation problem in the Mark I system, a set of studies of one alternate system had already been started reacting to the difficulty experienced in the K500 with the assumed 140 kV/cm maximum field. In these "Mark II" system studies, a set of magnetic dipole elements were introduced in place of the second electric deflector. These elements had much more bending strength than the electric deflector, reducing the magnetic field by 2 to 3 kilogauss along the extraction orbit whereas a 140 kV/cm electric field, if expressed in terms of an equivalent magnetic field, gives a reduction of only 800 gauss at the 200 MeV/nucleon maximum energy. When studies on the Mark I system uncovered the severe compensation difficulties in the K800 situation, the Mark II studies were discontinued since compensation for the elements assumed in that study would clearly have been very much more difficult than the compensation required by the Mark I system.

At this point, knowing the difficulty of the compensation problem, emphasis was shifted to a more pressing evaluation of the mechanical feasibility of extraction systems with perfect 3-sector magnetic symmetry. These considerations led to a compromise "Mark III" extraction system in

which the first two magnetic elements in the extraction system were replicated in every sector while the remaining extraction elements, which were further away from the internal beam, were to be compensated by a lumped element system as used in the K500 and in the Mark I K800 studies. Having become aware of the critical role of the extraction element fringe fields in determining internal beam behavior, we also at this point modified our numerical procedures into a "self-consistent" format, namely an iterative process was introduced in which, at the end, the elements used in producing the magnetic field for the internal beam calculation are identical to the elements used in the calculation of the extraction orbit. (A description and step-by-step example of the application of this process to the Mark IV extraction system is attached as Appendix A).

Results with the Mark III extraction system were successful in the aspect of providing adequate stability for the internal beam to survive various resonances, but a new problem, excessive phase slip relative to the accelerating voltage, was introduced by the rather large change in the average field in the internal beam region caused by the six, close-in extraction elements (the six elements being the two original elements plus the two compensator images of each of the original elements). This phase slip error was too sharp and too far out in radius for trim coil compensation -- it also could not be corrected by fixed changes in the steel configuration because of the relatively large range of variation of the extraction radii (approximately 1") required for the broad array of particles and energies which the K800 is expected to accommodate.

A "fix" for the Mark III phase slip problem was however developed, this being to introduce a "front porch" on each of the six innermost extraction elements, the front porch consisting of small bars of iron mounted on the

inner edge of the extraction elements just above and below the internal beam space. These added bars strengthened the magnetic field just inside the extraction element and thus reduced the phase slip. Since the front porch was attached to the extraction elements, it moved in and out as the extraction elements were moved for various beams, and the compensation therefore always occured at just the place where it was needed.

Computer studies of the Mark III system were successful in the aspect of extracting the full range of K800 beams with magnetic fields calculated self consistently and with extraction voltages not exceeding 120 kV/cm. The geometry of this system however involved a major inconsistency, namely that the front porch on the first extraction element protruded into the accelerating gap in a manner which would cause the dees to spark. An azimuthal shift of the front porch away from the accelerating gap was considered, but was not further explored due to both perceived mechanical difficulty and to flow of design interest to a more effective solution of the difficulty which is the Mark IV system.

The Mark IV extraction system differs from the Mark III in that the first magnetic extraction element, the element which infringed on the accelerating gap, is eliminated and the effect of this is compensated by making the second element longer and stronger and with two independent radial parts. One of these independent radial elements acts on the beam as it exits the first electrostatic deflector while the second affects the beam as it exits from the second electrostatic deflector.

The Mark IV extraction system constitutes a significant landmark in that for the first time all desired beams from the K800 are successfully extracted with electric fields of 120 kV/cm or less and with the location of all elements compatible with other cyclotron components. The magnetic

fields used in the calculations are also fully self consistent. A feature of the Mark IV system which gives concern is the tight aperture for the beam in the front porch area, where iron bars are located within 150 mils of the median plane. Studies including nonlinear effects indicate that a phase space distribution of adequate size can pass through the Mark IV system, assuming perfect alignment of all elements, but the tight alignment requirements are clearly a source of concern and an undesirable feature of this system. The Mark IV system is, nevertheless, a possible extraction system which could be used in the cyclotron, with appropriate care in construction, and for this reason the computer studies of this system are documented in this report.

Concurrently with preparation of this report, extraction studies have moved on to analyze a Mark V system which could be described as a combination of Mark II and Mark IV concepts. In this system the second electrostatic deflector (E2) is shortened to one-third of its original length and a magnetic dipole of form similar to those used in the Mark II system is introduced in the space previously occupied by the second one-third of the electrostatic deflector. This gives adequate extraction strength so that the third one-third of the original E2 space can be used for mechanical supports for the cryostat wall, thus eliminating the need for a complicated spring support system which is an implied essential feature of the Mark IV design.

Desirably the K800 extraction studies will ultimately be extended to a number of other cases before final freezing of design decisions. Progress in this direction will be expedited when new faster computer codes, which are in preparation, come into use. Also, all calculations to date have used computed magnetic fields, since processing of the data from the first

mapping cycle on the magnet has not yet been completed -- as soon as this data is available a transition to studies using measured fields will be made. Spot comparisons which have been made between the computed fields and the measured maps imply that changing to measured fields will have relatively minor effect on results such as those presented here.

III. Geometry of the Mark IV Extraction System

The Mark IV extraction system involves 14 clusters of magnetic bars capable of being independently moved in radius. Three of the clusters also have an adjustable angle of tangency, where the angle of tangency is defined as the angle between the centerline of the element and the tangent to a circle about the cyclotron center. In addition to the magnetic elements there are 2 electrostatic deflectors -- the first extending from 31° to 90° in the polar coordinate system of the cyclotron and the second extending from 151° to 210°. The computations assume that each of the electrostatic deflectors can be freely moved in radius and that the curvature can be adjusted such that the electric field is effectively always perpendicular to the orbit. Location of this array of elements is indicated schematically in Figure 1. Considerable mechanical complexity is clearly involved in the three locations where independently adjustable elements are located at the same azimuth, and this problem is further exacerbated by the fact that these elements also include the need for adjusting the angle of tangency. Mechanical studies of a drive system meeting these requirements have not been made -- qualitative evaluation of the situation leads to the conclusion that the design of an appropriate system would be difficult but not overwhelming. (The elements involved in the superposition are unfortunately

also ones with very small vertical aperture, as indicated further on, and the drive system must therefore also provide accurate alignment which adds significantly to the complexity of the required mechanical system).

Figure 2 shows the operating regime of the K800 cyclotron in a display in which the coordinates are the magnetic field at the center of the cyclotron in kilogauss and the charge to mass ratio of the ion to be accelerated. The working region of the cyclotron is shaded with boundaries indicated by heavy dashed lines and with internal solid and dashed lines within the shaded regions showing particular ions and various values of the final energy per nucleon. The extreme requirements on the extraction system occur on the boundaries of the operating region, the high and low energy boundaries giving separate extremes on the range of radial adjustment of the extraction elements and the high energy boundary giving the extremes of field strength. Six points in this space, corresponding to six different particle/energy combinations, have then been selected as representative of the extremes of the extraction problem. These six points are marked by heavy circles on the diagram with arrows indicating computer run labels for each of the points. (The computer labels are a shorthand combination of either the central magnetic field or the particle energy for the first digits and the ion charge to mass ratio for the final digits, i.e. 2005 is the computer designation for 200 MeV/nucleon with a charge to mass ratio of 0.5, 472 is the computer designation for runs at a central field of 47 kilogauss and charge to mass ratio of 0.2, etc.)

Table I gives the optimized azimuthal and radial location for each of the magnetic extraction elements for each of the six reference beams which are used in the analysis. Geometrical details of each element are shown in Figures 3 through 8, including the angle of tangency for each bar cluster

relative to the radius vector, except for the first cluster where the angle of tangency is variable (the specific setting of this angle for each beam in Table I). The magnetic field produced by each of the bars is approximately indicated in Figure 9 (the figure specifically showing the magnetic field which would be produced by each set of bars if the bars were infinite in length).

The M1 bar set functions as a "septum" magnet giving an abrupt field change of approximately 2 kG from the internal beam region to the extraction orbit path, the location of these orbits being marked by arrows in the M1 section of Figure 9. Bars M2 through M9 are primarily focusing elements -- the iron segments in these bars are then arranged to give linear field gradients of various strengths across the extraction orbit aperture. Bars designated C1 and C2 are used to compensate for the magnetic perturbations from the combined M3 through M8 group (the perturbations from M1 and M2 are compensated by their 120° images; the front porch on M1 brings the total change in the average magnetic field within the range of the trim coil system).

The main magnetic field which is used for these studies is computed in the "standard" way, using a two dimensional relaxation calculation to compute the field produced by an azimuthally averaged iron distribution and then using the saturation magnetization approximation to superimpose the effect of azimuthal varying elements on the base field obtained from the relaxation calculations. Table II gives a listing of the computer files containing the specific fields used for the studies in this report.

IV. Orbit Behavior -- Radial and Linear Axial

The iterative process by which a self-consistent extraction calculation is accomplished is described in Appendix A. This Appendix includes figures showing intermediate results as the design process converges to a self consistent solution.

The process described in Appendix A was used to compute extraction orbits for each of the other reference beams -- composite final results for all six beams are presented in Figures 10 through 13. Looking first at Figure 10, we see for each of the six reference beams (from top to bottom): 1) a bar graph showing the magnitude and sign of the currents in each of the 21 pole face correction coils; 2) the particle phase relative to the accelerating voltage; and 3) the axial focusing frequency plotted versus energy. Figure 11 gives a "tune diagram" for each reference beam, i.e. the radial focusing frequency plotted versus the axial frequency. Using this plot, possible problems with various resonances, which are shown as solid lines in the Figure, can be inferred. Figure 12 shows the "phase space" trajectory of the central ray of the internal beam for the last 50 turns of the acceleration process (once per revolution, radial momentum is plotted versus radius). The final turns of each of these trajectories show the beam to be off center and precessing, such that the radial step to the final turn is approximately 0.15 inches in each case. This precession was produced by using intentionally unequal currents in the outermost pole face coil on the three hills, thereby introducing a first harmonic field perturbation with amplitude and azimuth as indicated by the "bump" label on the drawing. (The needed first harmonic was determined as described in Appendix A so as to

connect centered orbits prior to extraction onto an orbit making the desired 0.15 inch radial jump at the electrostatic deflector entrance.) The very substantial variation in extraction radius shows clearly in the Figure.

Figure 13 shows the behavior of families of trajectories passing through the extraction system. The plots include both radial (x) and axial (z) displacements. For each beam, the active extraction elements are marked on a "box" graph between the two displays, the absence of a box indicating that the element is removed. The groups of rays for the four beams which represent the high field limit of the accelerator are well behaved. The two low field beams display growth in both z and r but are within the aperture limits of the system for emittances of 5mm-milliradians radially and 20mm-milliradians axially.

Linear studies of the axial motion of the internal beam showed no appreciable beam growth for any of the cases presented here. (A prior step in the calculation of the 1405 case gave a significant axial blowup of 2-3 fold in the final turn with an extraction system which differed from the one described here only in the characteristic of having the M1 radius shifted by 0.07 inch -- this is an indication of the very tight alignment tolerances which would be involved in an actual extraction system based on the Mark IV design.)

V. Axial Motion Including Nonlinear Fields

Several of the iron elements of the Mark IV extraction system are located very close to the median plane (see Figure 3). This then implies the probability of strong nonlinear components in the field -- such components could introduce severe distortions in the phase space volume

occupied by the beam which would enlarge the practically useable beam emittance and/or produce beam losses in the extraction channel. To study this problem a special code was prepared which computed exact fields both on and off the median plane for all magnetic elements in the extraction system, using the assumption that all magnetic dipoles in the bars are fully aligned in the axial direction (this being an assumption which should be quite accurately valid at the high field levels involved in the K800). The special code also includes the leading nonlinear term in the background field produced by the main magnet and the trim coils (since all of these elements are far from the median plane relative to the extraction elements, the leading term should be the dominant contribution in the non-linear beam phenomena). Results of these studies are shown in Figures 14, 15 and 16.

Figure 14 shows a study of the effect of the $\nu_r = 2\nu_z$ coupling resonance in the 1203 field. In this study a central ray starting point was picked as a point ten turns before the coupling resonance for the trajectory from Figure 12. At this central ray energy 12 displaced rays were set up as indicated by the diagrams at the top right in the figure--the four points on the radial eigen-ellipse are coded as squares, diamonds, vertical crosses, and slanted crosses--for each of these three (z,p_z) trajectories are computed namely (0,0), and a pair of (z,p_z) values corresponding to the end points of the two semi-axes of the axial eigen-ellipse, the later pair plotted as solid and dotted lines in the Z vs. turn number plot. (The median plane symmetry makes opposite ends of each semi-axis identical so that tracking of these rays is unnecessary.) All rays were run forward through the resonance until they reached the deflector entrance, the locations of the various rays in the radial phase space being as shown in

the lower part of Figure 14 with the axial motion as shown at the upper left. (In both of these plots the $(z_1,p_2)=0,0)$ rays are omitted except the final turn values are plotted as heavy dots in the (r,p_r) graph.) Inspecting these results we see that three or four of the rays show an appreciable increase in z amplitude, one shows a significant decrease, and the remainder a moderate decrease. The increase in axial amplitude is however in a range which is acceptable. Noting that the coupling resonance converts radial amplitude into axial amplitude, we conclude that the group of rays was centered sufficiently well at the resonance. Details of the coupling of the axial motion into the radial motion show in the lower graph of Figure 14. In this plot the central ray of the whole group is indicated by the points connected with a solid line -- the pair of orbits with z displacements are plotted, a particular symbol designating the particles associated with a particular turn, and as noted above, for the last turn solid dots have been added to show the locations of the rays with zero z amplitude at each value of the radial amplitude. Overall, the results are reasonably acceptable. The points associated with the final turn are all seen to be at radii as large or larger than points associated with any previous turn, so that a very thin septum at approximately 40.363" would cleanly divide the internal and external beams. (This clean separation of course could be smeared if a broad range of rf phase was occupied as is usually the case in a heavy ion cyclotron -- in this circumstance the extraction becomes statistical with 50% being the typical efficiency of a well designed system.)

Noting that the 1405 operating point displayed sharp sensitivity to the position of the M1 bar in the linear axial motion studies described in Section III, an additional set of nonlinear axial motion runs were made to

see whether results for this operating point would be significantly different from those for the high field operating point presented in Figure 14. Figure 15 and 16 then give results similar in form to those of Figure 14 except that the operating point is 1405 and only the six turns immediately prior to extraction have been tracked. Also, two different values of the z emittance have been included, namely, 5mm-milliradians in Figure 15 and 20mm-milliradians in Figure 16, in order to observe the dependence of the coupling on emittance. Results for both values of the emittance are seen to be rather well behaved, i.e., no special problems come up with this operating point other than the previously mentioned sensitivity to bar position.

Figure 17 shows results when the nonlinear codes are used to track the extraction orbit for the high field case. The output format is unfortunately different from that of the linear code, but nevertheless, a visual comparison of the envelope results for z and x at the right of the figure versus the linear results from Figure 13 gives a clear indication of the close agreement between the results of the two calculations. This is more quantitatively evidenced by the emittance plots at the right in Figure 17, where the solid lines give the ellipses resulting from the linear motion whereas the clusters of points about the elipses reflect the fuzzing out of the boundaries due to the linear and nonlinear couplings. These effects are however in each circumstance quite moderate and the overall behavior is clearly acceptable.

VI. Conclusions

The Mark IV extraction system has been numerically evaluated at each of six operating points spanning the operating regime of the K800 cyclotron. The overall behavior of the extraction system from a perspective of orbit dynamics is reasonable. The evaluation is based on fully self consistent analysis and includes full nonlinear effects of the extraction elements.

The one significant shortcoming in this study, namely that the rf phase has in every case been taken to be the design value rather than scanning a spread of phases, is necessitated by the very large amount of computing which is involved in the evaluation of such a system. Previous studies, in less complicated situations, of the effect of a non-zero rf phase width support with considerable confidence the expectation that a search on rf phases would simply introduce a smearing of the results presented here and a lowering of the extraction efficiency to something in the vicinity of 50%. Our design plan is to proceed with evaluation of a number of possible extraction systems to the point where they can be compared with the Mark IV results presented here and, for the most promising of these systems, a search on rf phase will be added to fully confirm the final result.

APPENDIX A

Finding Extraction Element Positions in K800 Fields

A main field without focusing bars is generated with the trim coil fitting program (current version TCFIT805). The phase curve to be fit is made up by hand, and modified until coil currents and focusing are reasonable. One fitting run takes about eight minutes on the VAX 11/780. Results can be plotted by the program FITPLOT.

The deflector program (currently DEFIN801) is used to find an extraction path, using a fixed displacement from the final equilibrium orbit to supply the deflector-entrance beam position. Since the orbit used for a guess does not take focusing-bar fringe fields into account, the displacement used must be based on experience with other fields. The deflector program is interactive, with graphic output showing beam position relative to the focusing bars. It is usually easiest to start with only the first two bars and their harmonic compensators calculated as assemblies of charge sheets, leaving the rest in a lumped parameter representation (bias field and gradient automatically centered on the orbit). The locations of the first two bars and the deflector voltages are then adjusted to bring the beam out in the desired direction. Because the harmonic compensators (which must move along with the focusing bars) influence the beam path, this adjustment is a slow, trial-and-error process. The two electric deflectors are usually kept equal, to eliminate one parameter. After a good beam path is obtained, the constant-field bars are changed to the charge-sheet form, and placed so as to give the same path.

The focusing-bar locations found by the deflector program are used to calculate a polar grid of fields in the internal beam space. Since the fringe field of the bars increases very rapidly at large radii, the grid has smaller radial steps there (usually 1/16" for the range 38-42"). The fitting program computes an average of the three sectors for use by its internal equilibrium orbit routine. The calculation of this bar field is done by the program CHGFLD2 and takes about ten minutes on the VAX.

A new main field is generated, including the focusing-bar fringe field. The given phase curve (points marked in Fig. 18 center) may not be very well approximated by the fit (solid line in Fig. 18 center). If the difference is too large, currents will get out of control, and the phase curve must be changed. This is usually done by fixing the outermost trim coil at a reasonable value and using the final negative-to-positive phase swing (transposed up or down if necessary) as part of the new curve.

The new main field is combined with the previously computed bar field to make a two-part polar grid with small radial steps at the edge of the pole. Interpolating in this table is almost as fast as it would be in a normal main-field grid, a critical factor in the accelerated orbit runs. The program which makes this grid is called CHGFLD1 and takes about one minute.

An accelerated orbit is run backward from the deflector entrance, using an interactive version of Spiral Gap (called SPRGAPI1) and the new two-part field. The initial r and p_r are adjusted to give the smallest radial-oscillation amplitude which will provide 0.15" of turn separation for extraction. Then the trim coil bump (first and second harmonics) is adjusted to give near-zero amplitude fifty turns back.

The deflector program is run again, using initial conditions from the accelerated orbit (r, p_r at the deflector entrance) and the new main field (not the version with the bars added -- the deflector program computes its own bar fields). The focusing bars will generally need to be moved from 0.01 to 0.05 inches.

Since the bar positions have changed, a new main field fit and a new accelerated orbit must be run. It will then usually be possible to run the deflector program with the bar positions unchanged, adjusting only the deflector voltages to make the beam follow the correct path. If not, the process must be repeated. This gives a self-consistent solution to the extraction problem, that is, a calculation in which the same magnetic field is used for both internal and extracted orbits.

A plotting program (called EXSYSPL1) uses output files from the last accelerated orbit and deflector runs to make drawings of the various magnetic elements with the extracted ray and the maximum radius of the internal orbits shown. This is the easiest way to check clearance. If a focusing check is desired, the equilibrium orbit program (this version is called GENSPE1) is used to obtain invariant ellipse parameters at the deflector entrance. This program uses the field file prepared for Spiral Gap. The invariant ellipse is entered into the deflector program to produce x- and z-envelope plots.

Typical results for the various steps of this process are shown in Figs. 18 through 29, the captions indicating the evolution of the design at various stages and the convergence to a fully self-consistent result.

TABLE I.--RADIAL LOCATIONS, M1r, M2r,...ETC. FOR THE FOCUSING BARS IN THE SIX REFERENCE FIELDS. FOR M1 THE ANGLE OF TANGENCY WHICH CHANGES WITH THE FIELD IS ALSO GIVEN. FOR OTHER M'S THE ANGLE OF TANGENCY IS FIXED AT VALUES INDICATED IN FIGS. 3 THROUGH 8.

Field	334.5 214.5 94.5° M1r	M1α	94.5 334.5 214.5° M2r	259.5° M3r	293° M4r	312° M5r	321° M6r	331° M7r	343° M8r	95° C1r	153° C2r
2005	40.950"	-1.7°	42.510"	out	44.257"	45.209"	45.895"	46.981"	49.037"	45.400"	43.700"
1416	39.995	-2.7	41.675	out	43.686	44.789	45.565	out	48.928	45.000	43.450
1203	40.785	-1.3	42.350	43.079	44.212	45.219	45.926	47.030	49.100	43.150	44.150
1405	40.585	-2.4	42.260	out	44.022	45.028	45.751	out	48.975	45.300	43.800
472	40.375	-1.5	42.050	42.794	44.033	45.102	45.842	46.988	49.115	42.950	44.000
1604	40.855	-1.5	42.397	43.096	44.214	45.208	45.910	47.007	49.068	43.300	44.100

TABLE II.--FILE REFERENCES FOR MAGNETIC FIELDS

1) SYS$VAXUSERS:[DJOHNSON.800FIT]K800FIT.DAT;2

This file was created on 3/18/85. It contains main coil fields, iron average fields for 35 excitations, trim coil average fields, trim coil resistances, and a dee width table.

2) SYS$SYSDEVICE:[DJOHNSON]K800MOD.DAT;2

This file was created on 6/16/83. It contains the iron azimuthal modulation data ("flutter").

3) SYS$SYSDEVICE:[DJOHNSON]K800TCBIN.DAT;1

This file was created on 6/17/83. It contains complete trim coil fields in unformatted binary.

All the above field files are in the form required by the fitting program TCFIT805.

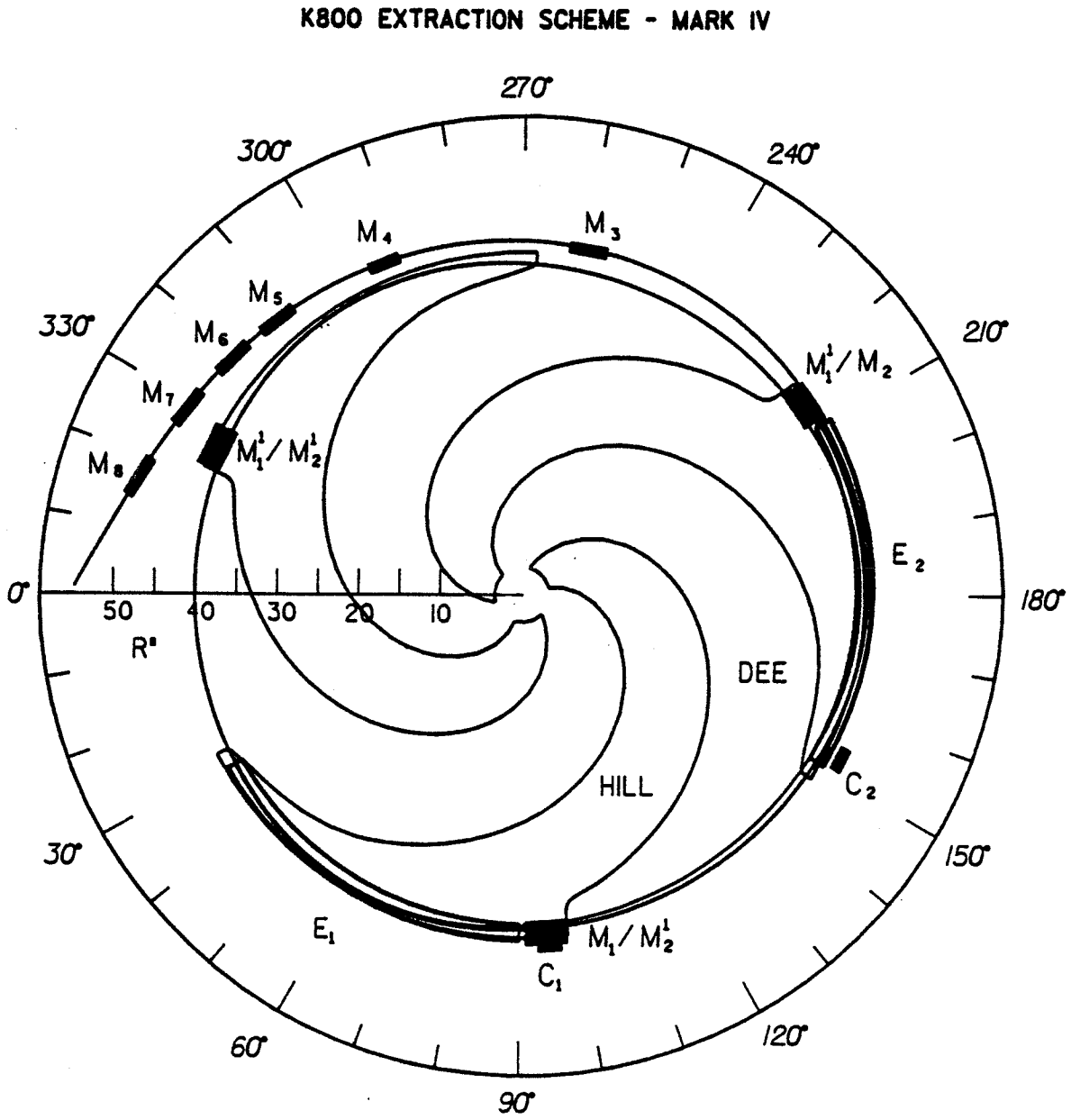

FIG. 1.--Schematic layout of the Mark IV extraction system for the K800 cyclotron. Electrostatic deflectors are labeled with "E", focusing magnet channels with "M". Exact Ccompensating bars are marked with X' other compensating bars are labeled "C".

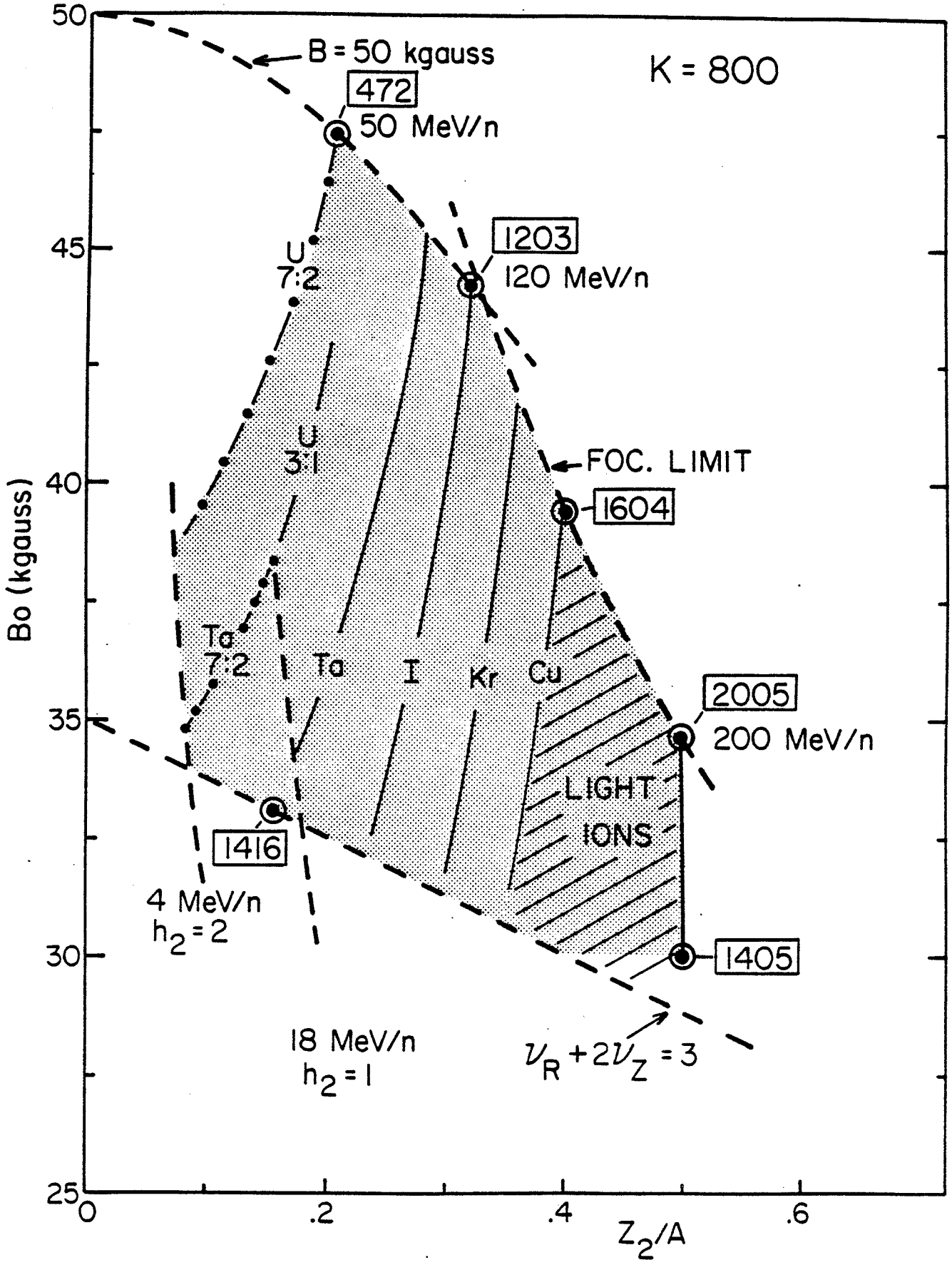

FIG. 2.--The operating regime of the K800 cyclotron plotted as central magnetic field, B_o, versus ion charge-to-mass ratio, Q/A. The labels in boxes indicate the computer run designation for the family of six limiting operating points, the circled dots, which are used for the extraction studies.

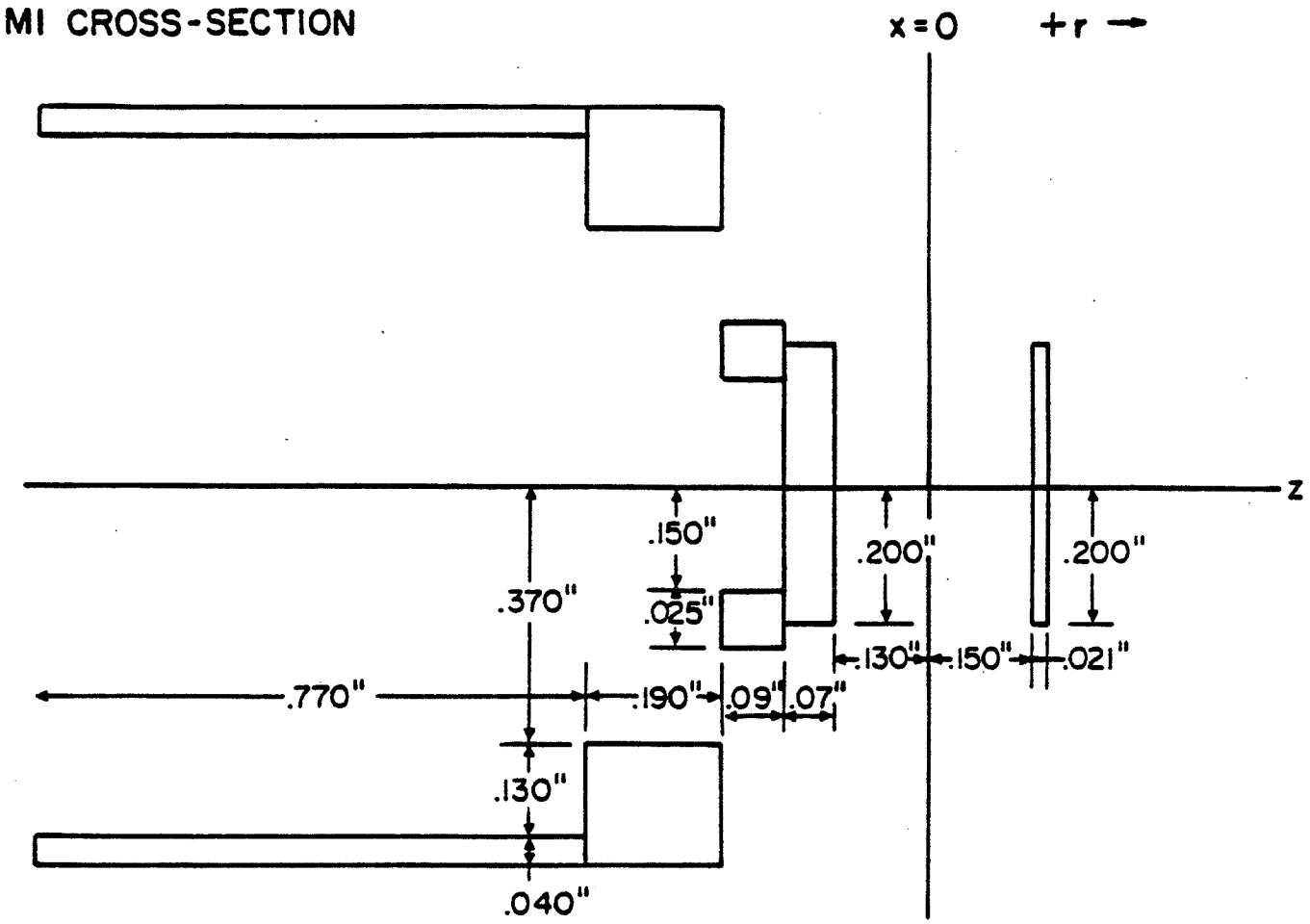

FIG. 3.--A drawing showing the cross section of the array of steel bars in the three magnetic extraction elements designated M1 and M1 compensators. All M1 iron elements are 5.14 inches in length. The three groups are centered at azimuths 94.5°, 214.5° and 334.5°. The radial location of the x=0 point and the angle of tangency are as indicated in Table I.

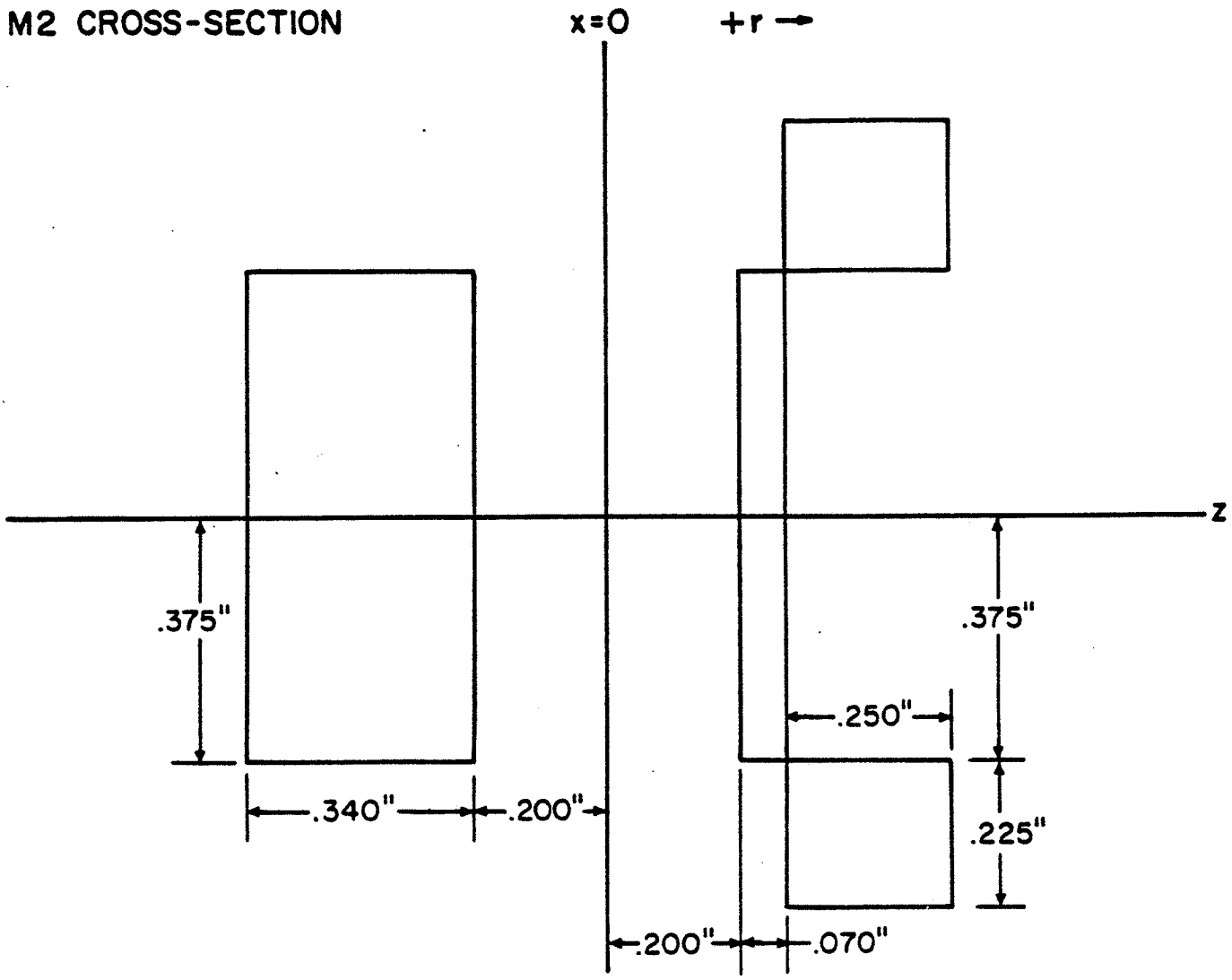

FIG. 4.--A drawing showing the cross section of the array of steel bars in the three magnetic extraction elements designated M2 and M2 compensators. All M2 iron elements are 5.14 inches in length. The three groups are centered at azimuths 94.5°, 214.5° and 334.5°. The radial location of the x=0 point is as indicated in Table I. The angle of tangency for all M2 bars is 0°.

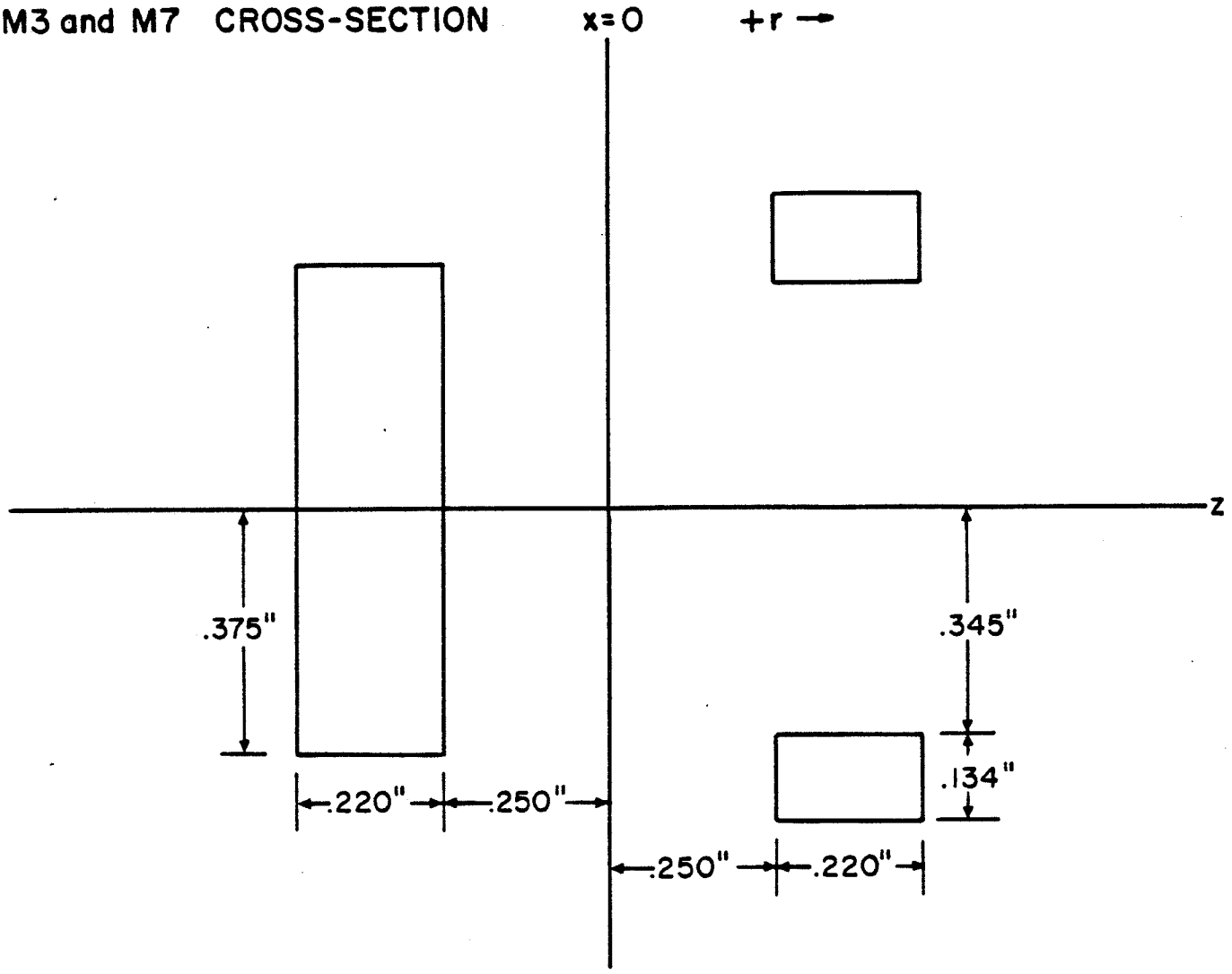

FIG. 5.--A drawing showing the cross section of the array of steel bars in the magnetic extraction elements designated M3 and M7. The length, angle of tangency, and central azimuth of the M3 bar family are 4.5", 1.9°, & 259.5° respectively. Corresponding quantities (for M7 are 4.92", 9.3°, & 331°. Radial locations are as indicated in Table I.

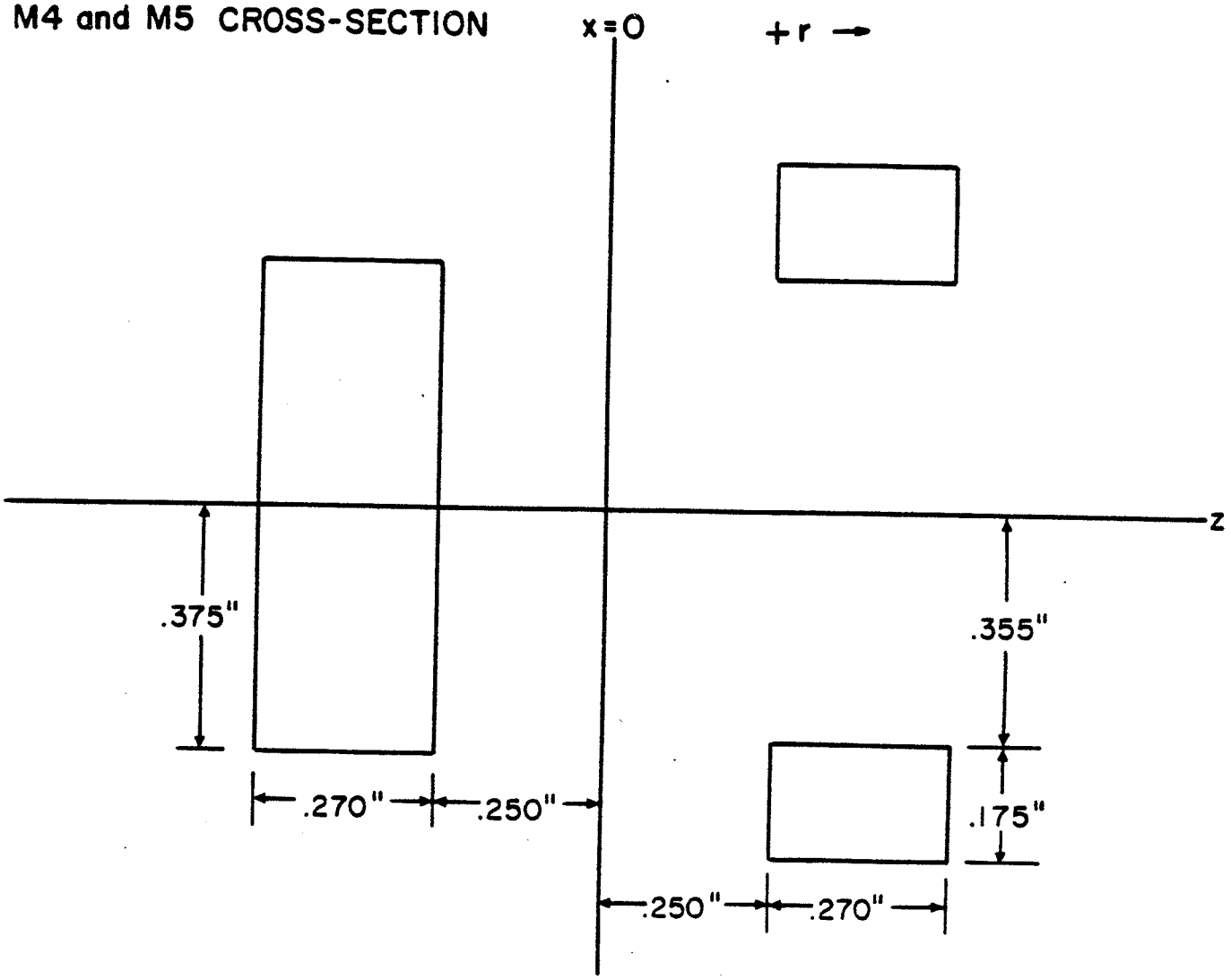

FIG. 6.--A drawing showing the cross section of the array of steel bars in the magnetic extraction elements designated M4 and M5. The length, angle of tangency, and central azimuth of the M4 bar family are 3.86", 3.4°, & 293° respectively. Corresponding quantities for M5 are 4.74", 5.2°, & 312°. Radial locations are as indicated in Table I.

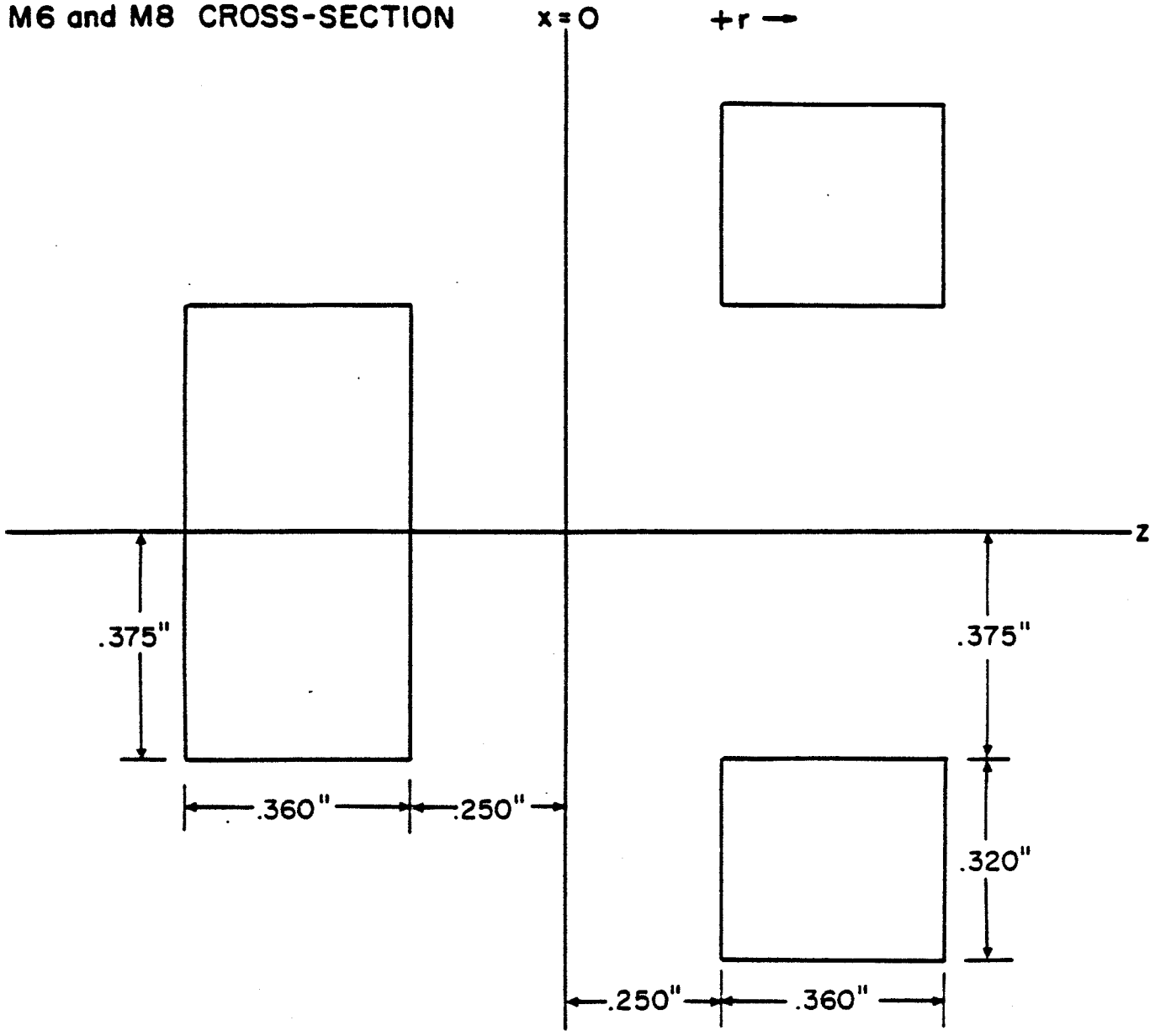

FIG. 7.--A drawing showing the cross section of the array of steel bars in the magnetic extraction elements designated M6 and M8. The length, angle of tangency, and central azimuth of the M6 bar family are 4.80", 6.9°, & 321° respectively. Corresponding quantities for M8 are 5.14", 14.9°, & 343°. Radial locations are as indicated in Table I.

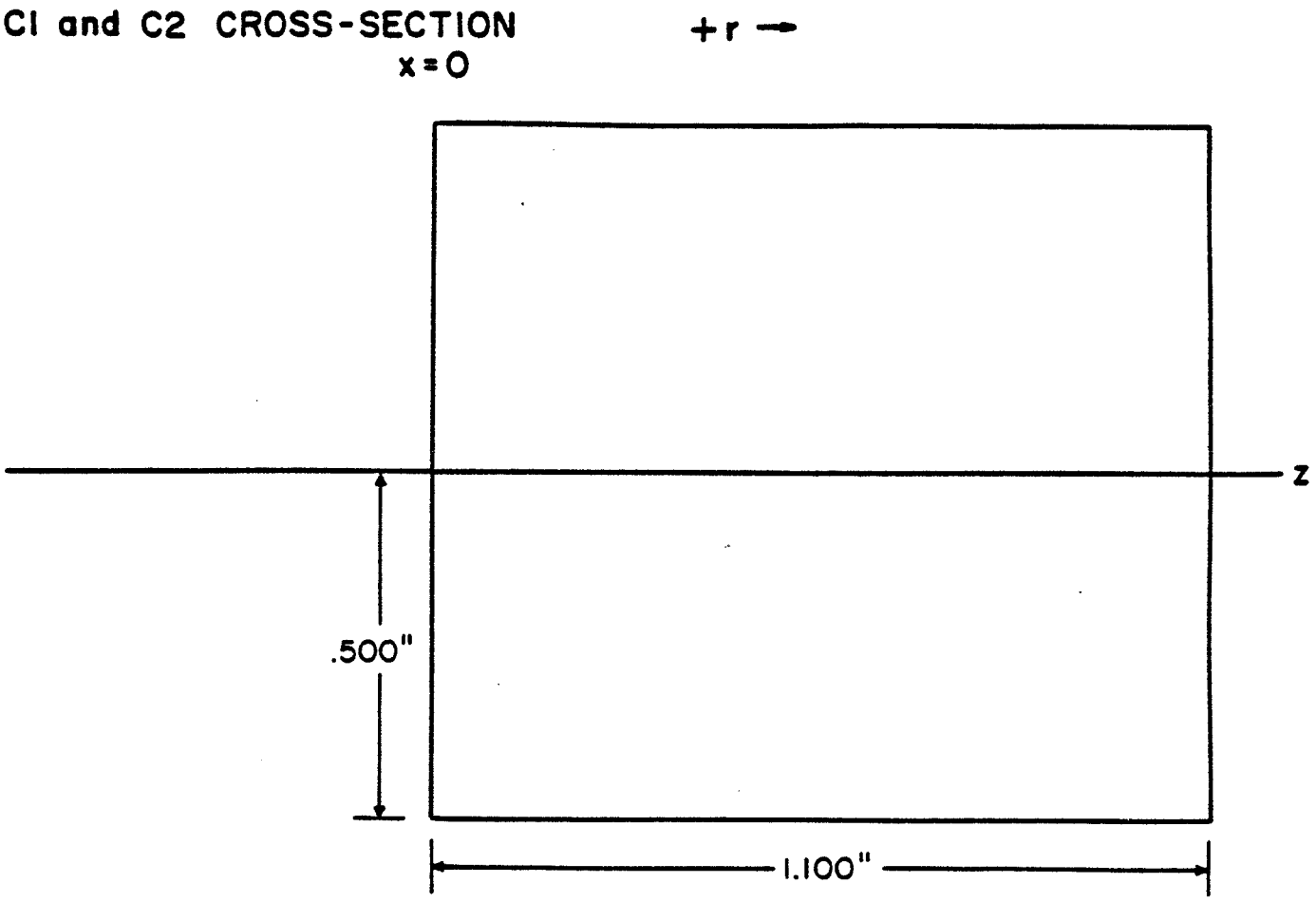

FIG. 8.--A drawing showing the cross section of the steel bars in the magnetic extraction elements designated C1 and C2. The length, angle of tangency, and central azimuth of the C1 bar are 2.88", 0.0°, & 95° respectively. Corresponding quantitites for C2 are 2.88", 0.0°, & 153°. Radial locations are as indicated in Table I.

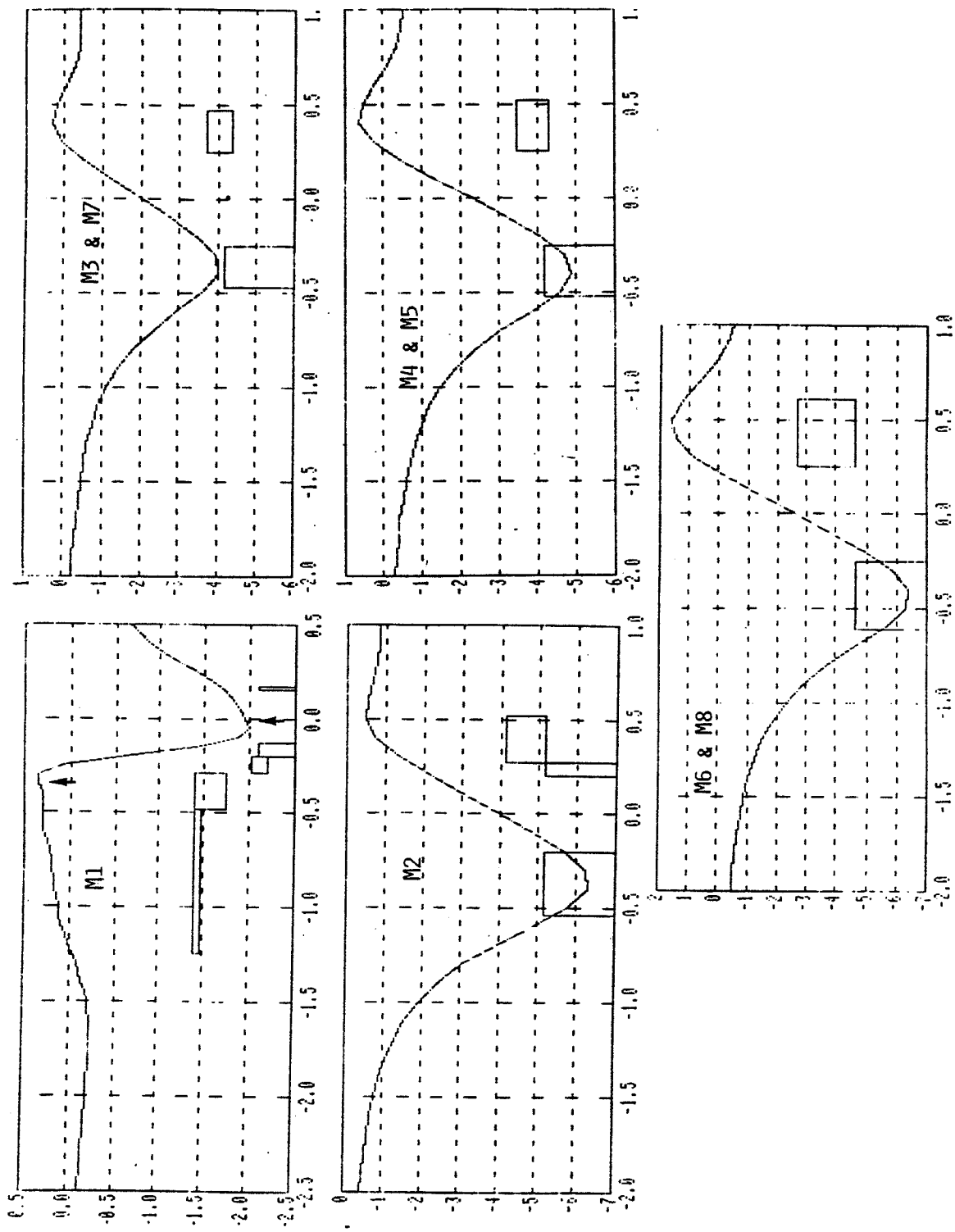

FIG. 9.--Magnetic field produced by iron bars of infinite length, magnetized in the z direction to saturation, and with cross section the same as the various focusing elements used in the Mark IV extraction system. The vertical scale is in kilogauss, the horizontal scale in inches. The outline of the iron bars is also shown on a scale in which the median plane is at the lower edge of each figure and the vertical linear dimension scale is the same as the horizontal linear dimension scale.

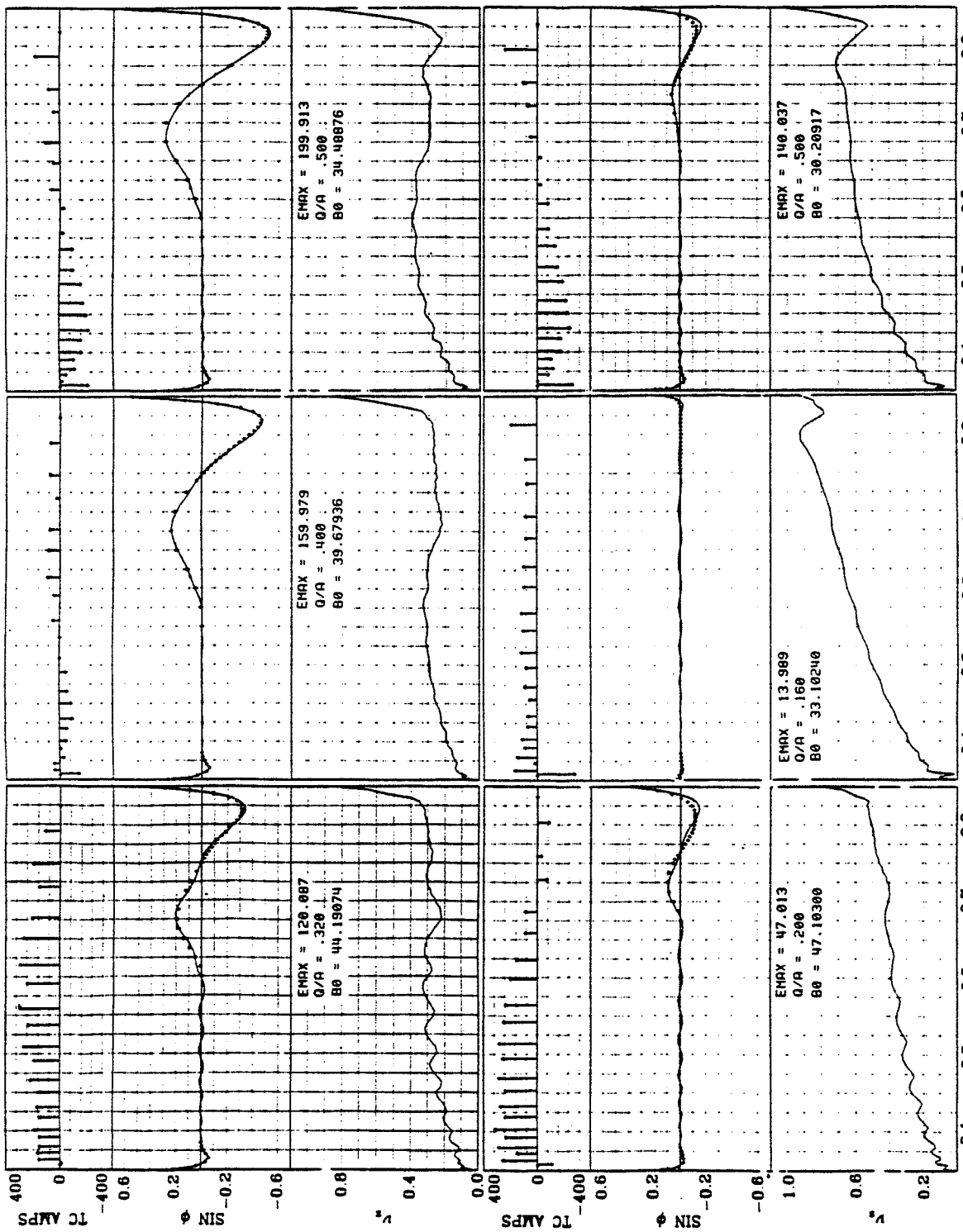

FIG. 10.--Results from the final run of the trim coil fitting code for the six referenced beams. For each beam the trim coil currents are shown as a bar graph at the top, the sine of the desired phase is plotted as a set of points at the center, the actual value of the sine of the phase in the computed field is plotted as a solid curve at the center, and at the bottom the axial focusing frequency ν_z. The horizontal scale in all cases is energy divided by maximum energy.

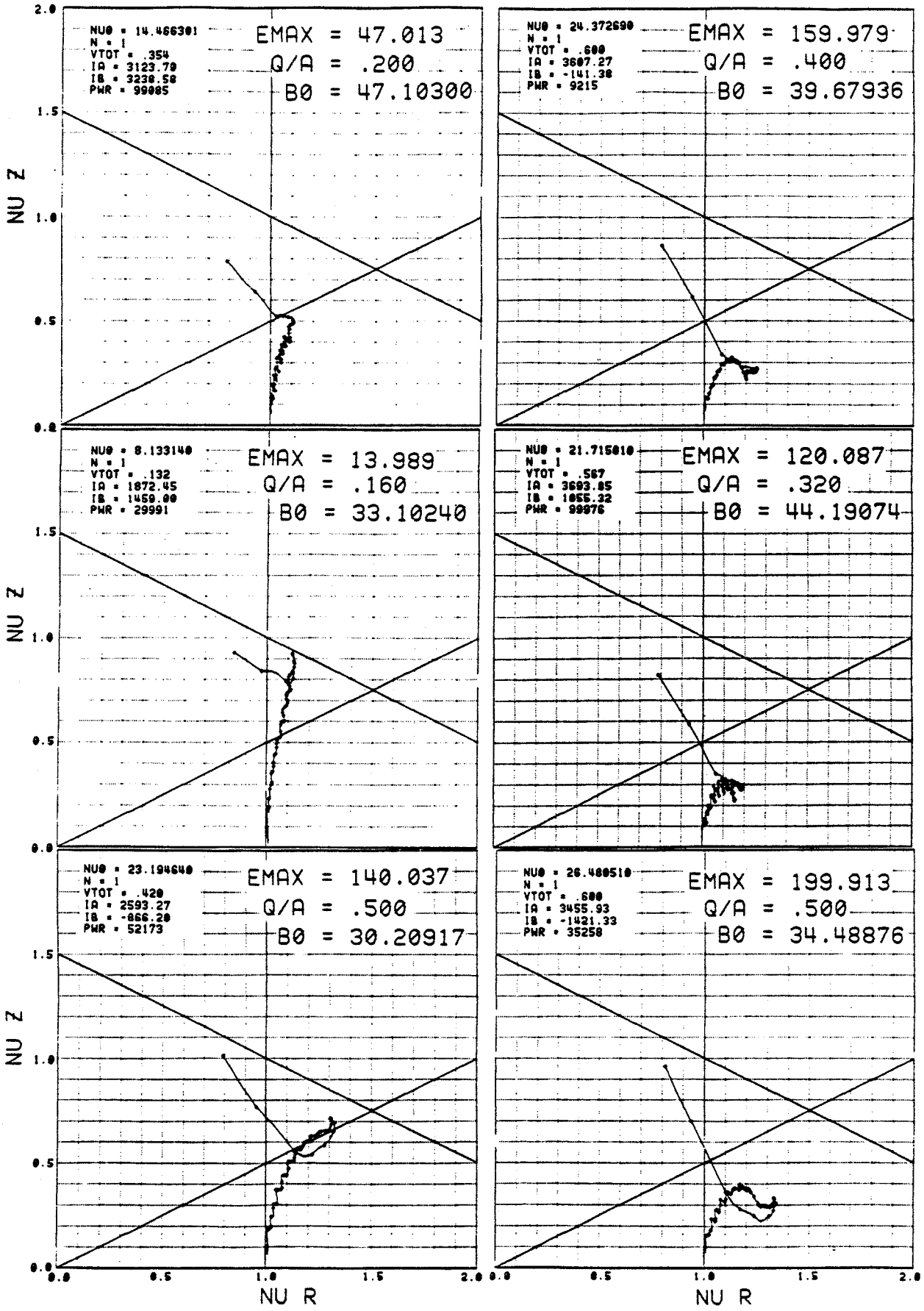

FIG. 11.--focusing frequency diagrams for the six reference beams with important resonances drawn in as solid straight lines.

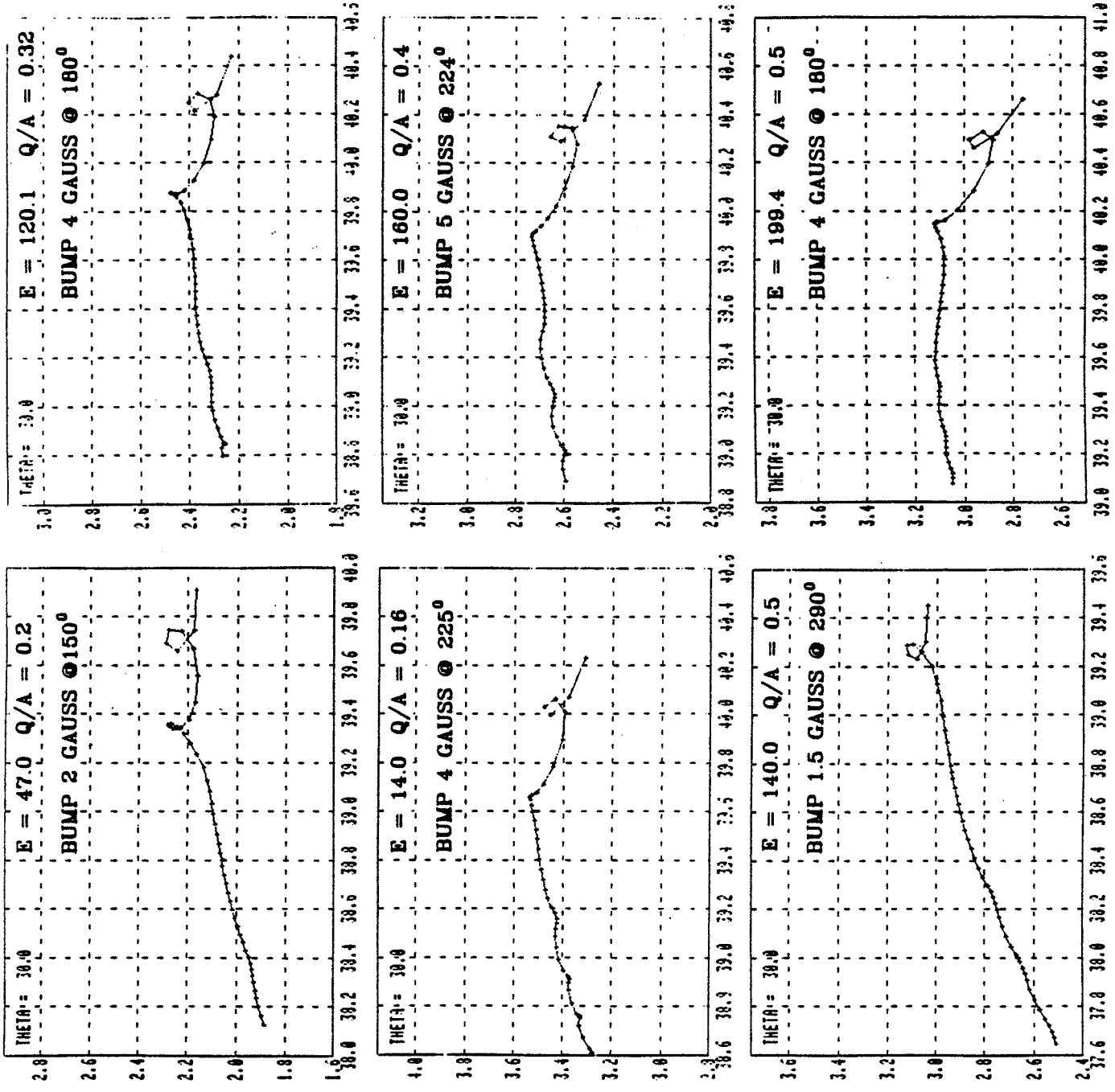

FIG. 12.--The final 50 turns of the selected central ray for each of the six reference beams.

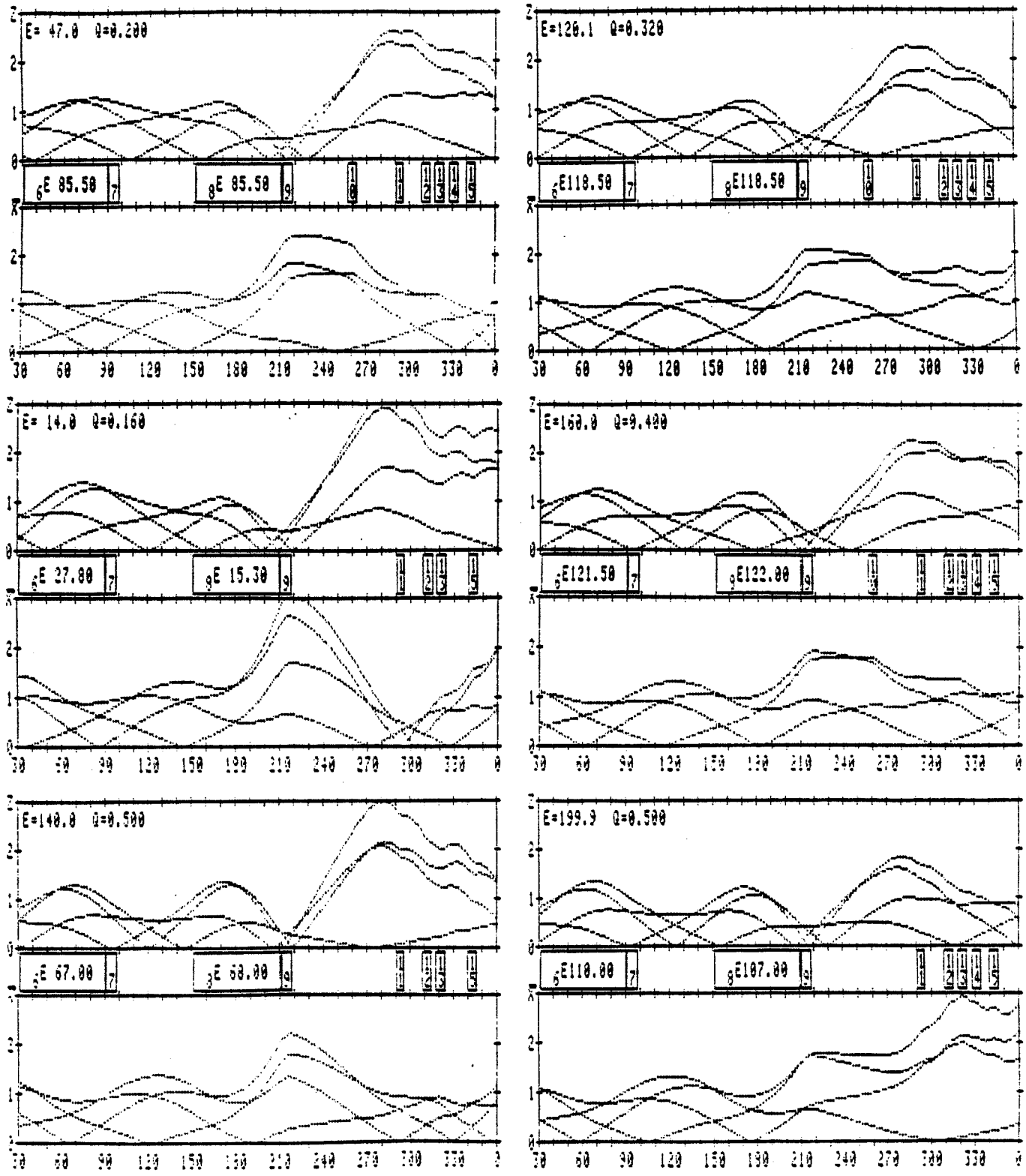

FIG. 13.--Linearized motion of families of orbits displaced in Z and X at the entrance of the first electrostatic deflector and tracked to the cyclotron exit. The behaviour is shown for each of the six operating points.

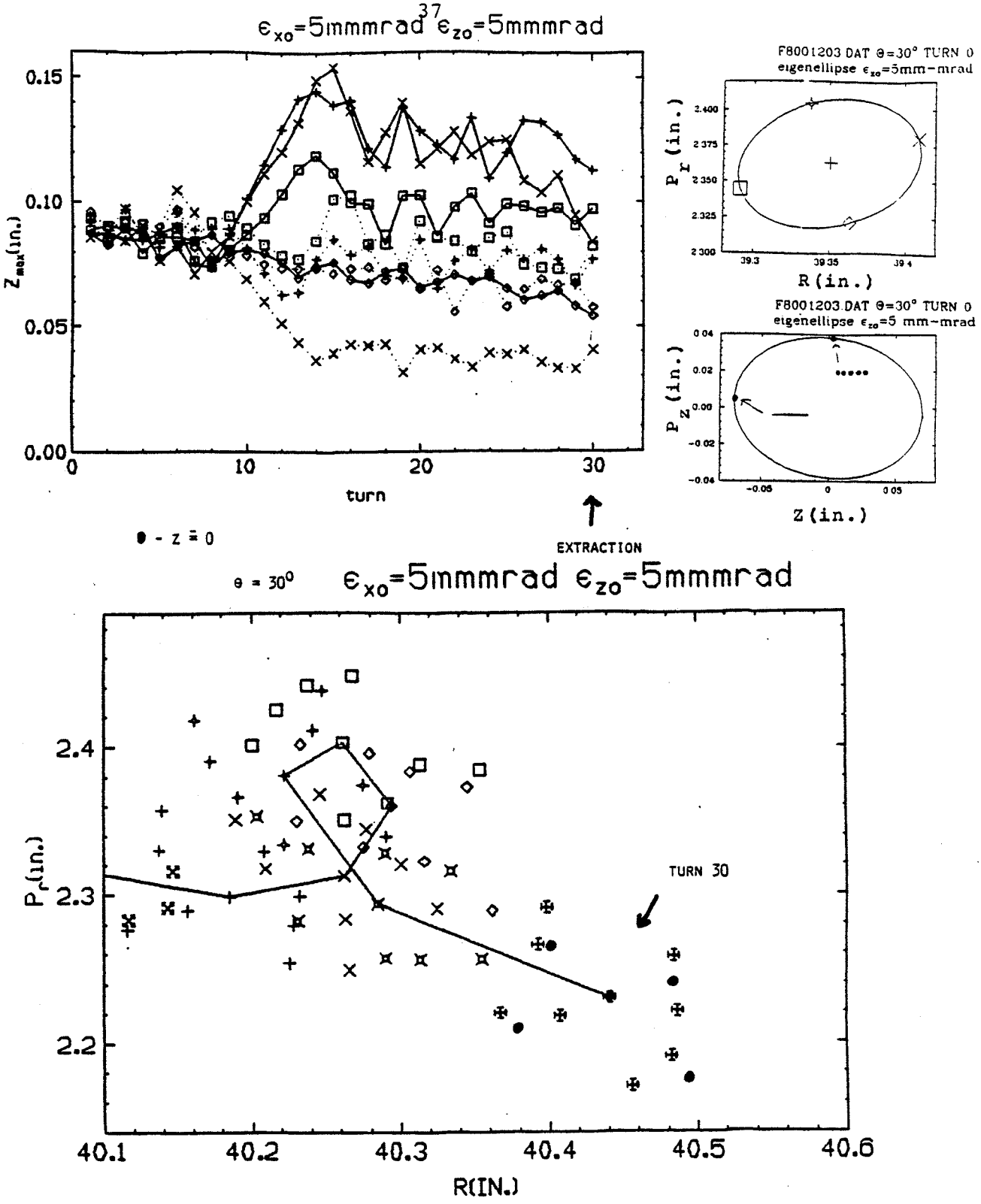

FIG. 14.--Study of beam behaviour in the resonance region at the edge of the 1203 field. Off median plane fields are computed exactly for the focusing bars and to fourth order in z for the main magnet and coils. (See text.) Initial conditions are shown at the upper right for r & z. At the upper left the maximum value of |z| in each revolution is plotted, the coding of the curves being as given in the initial condition plot. At the bottom the radial behaviour of the various rays is plotted once per revolution on radial momentum vs. radius axes. In this plot points on a given turn are indicated by a given symbol, with the coding defined by the central ray points which are connected by the solid line.

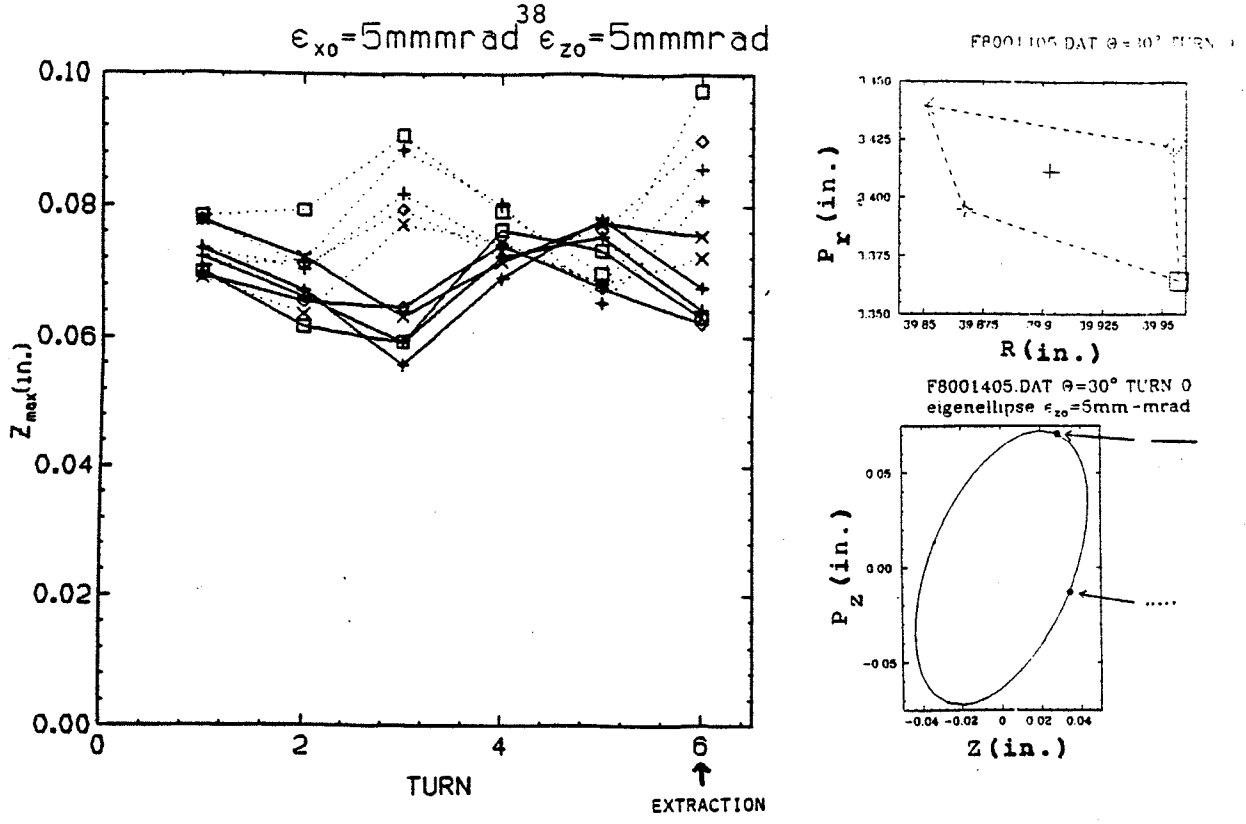

• - z = 0

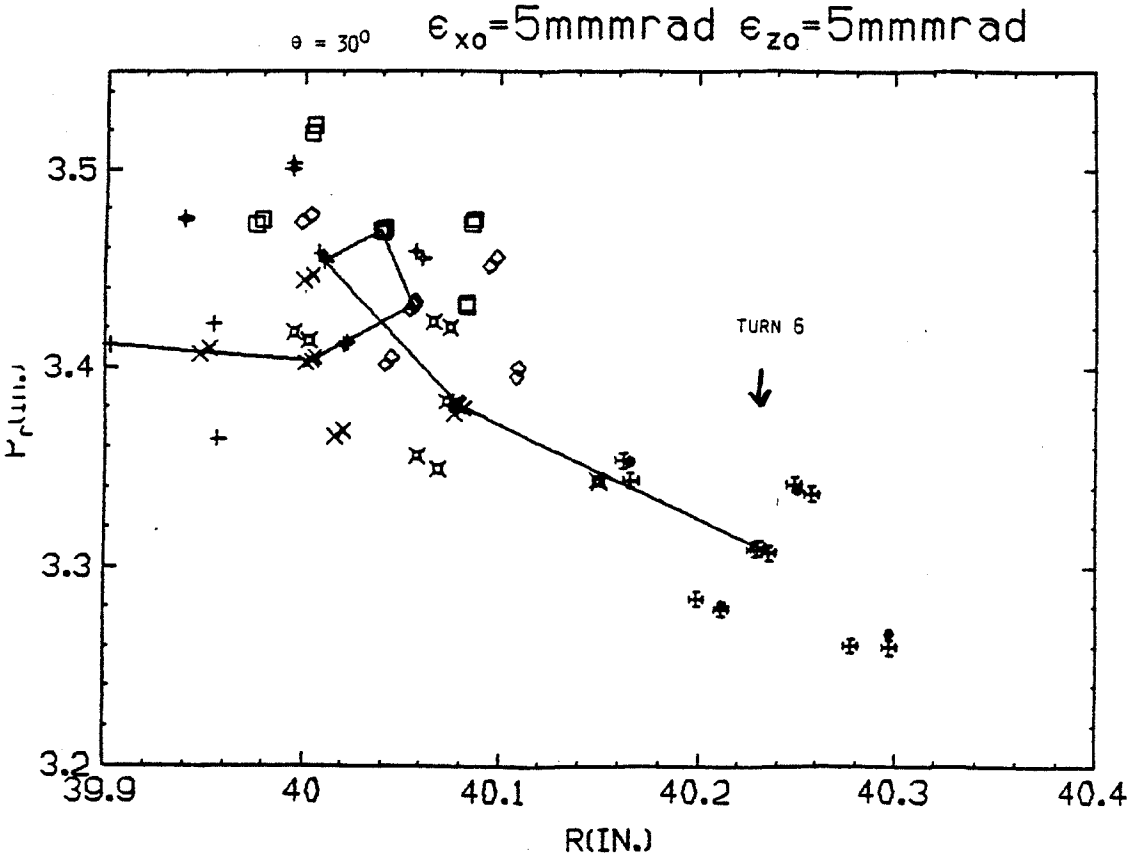

FIG. 15.--A study similar to that of Fig. 14 but in the 1405 field.

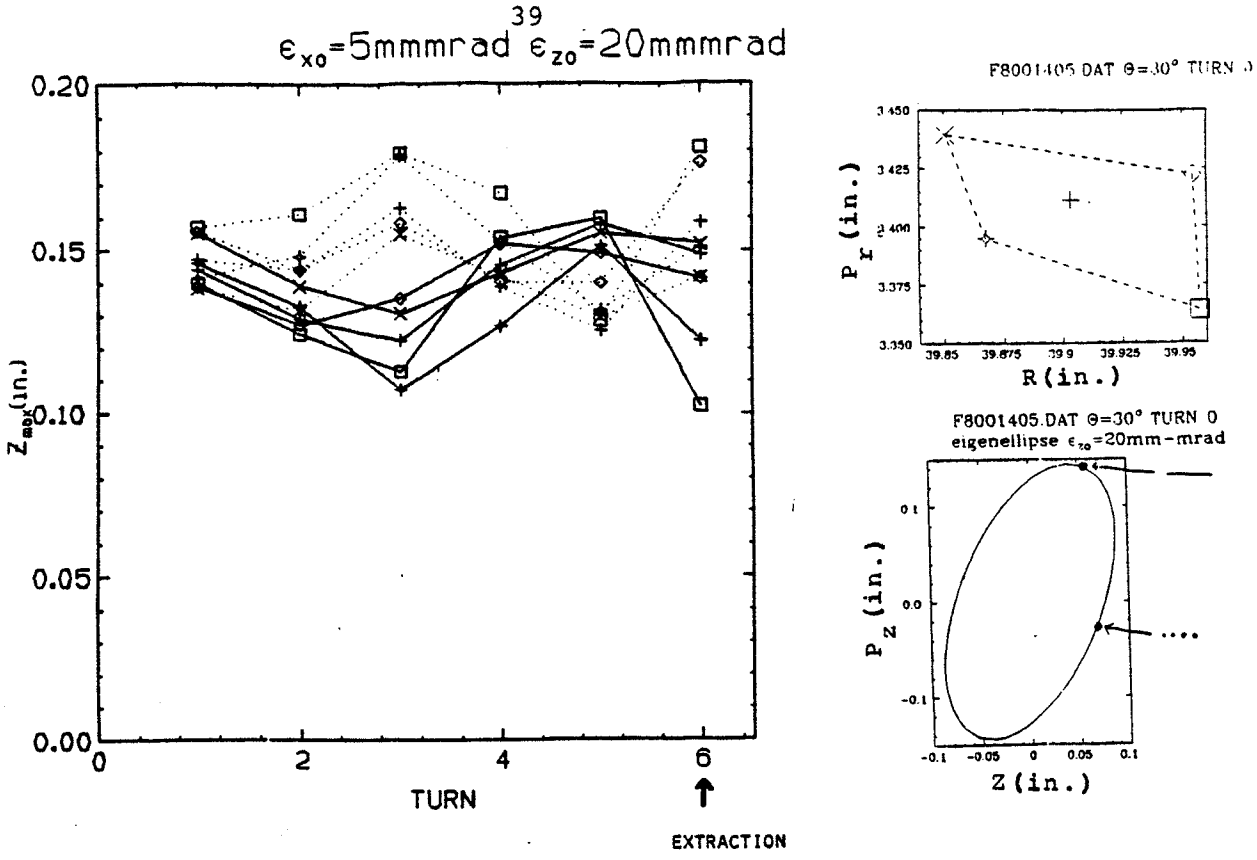

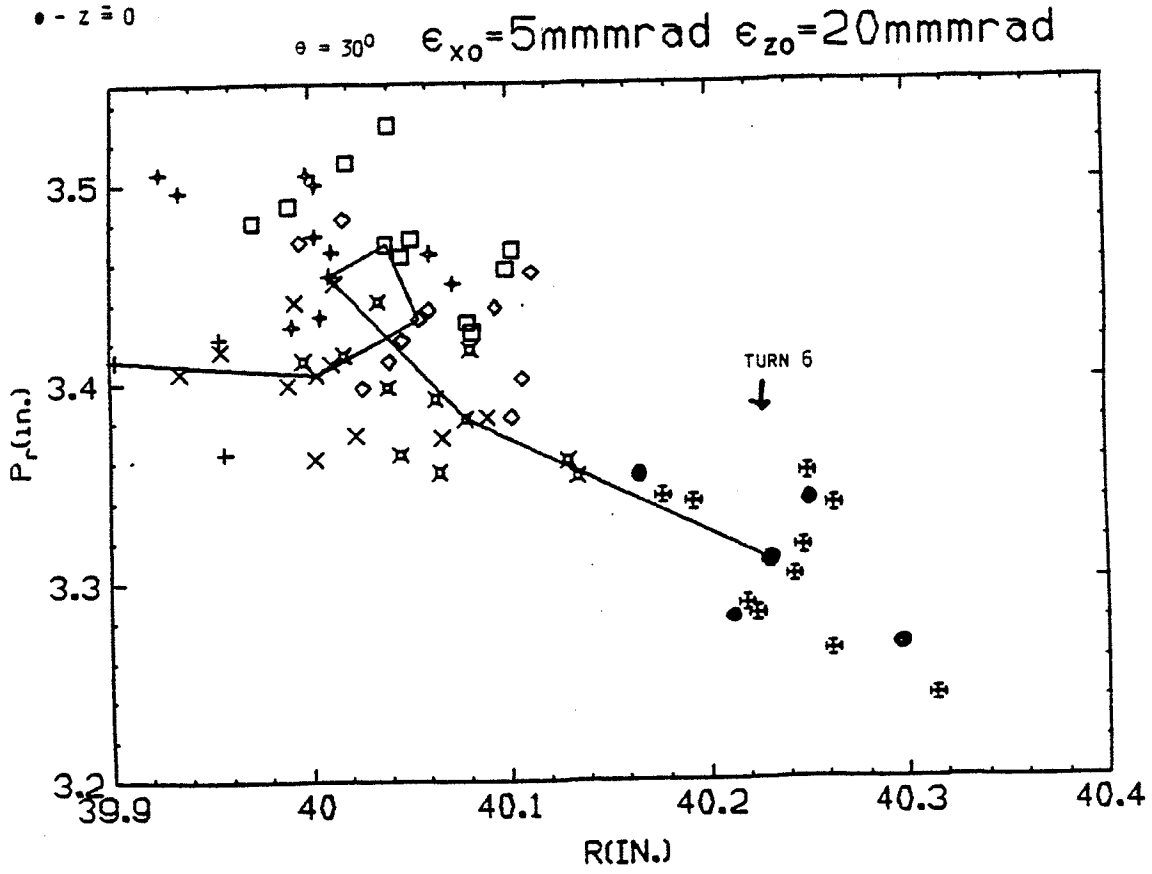

FIG. 16.--A study similar to that of Fig. 15 but with the axial emittance expanded to 20mm-milliradians.

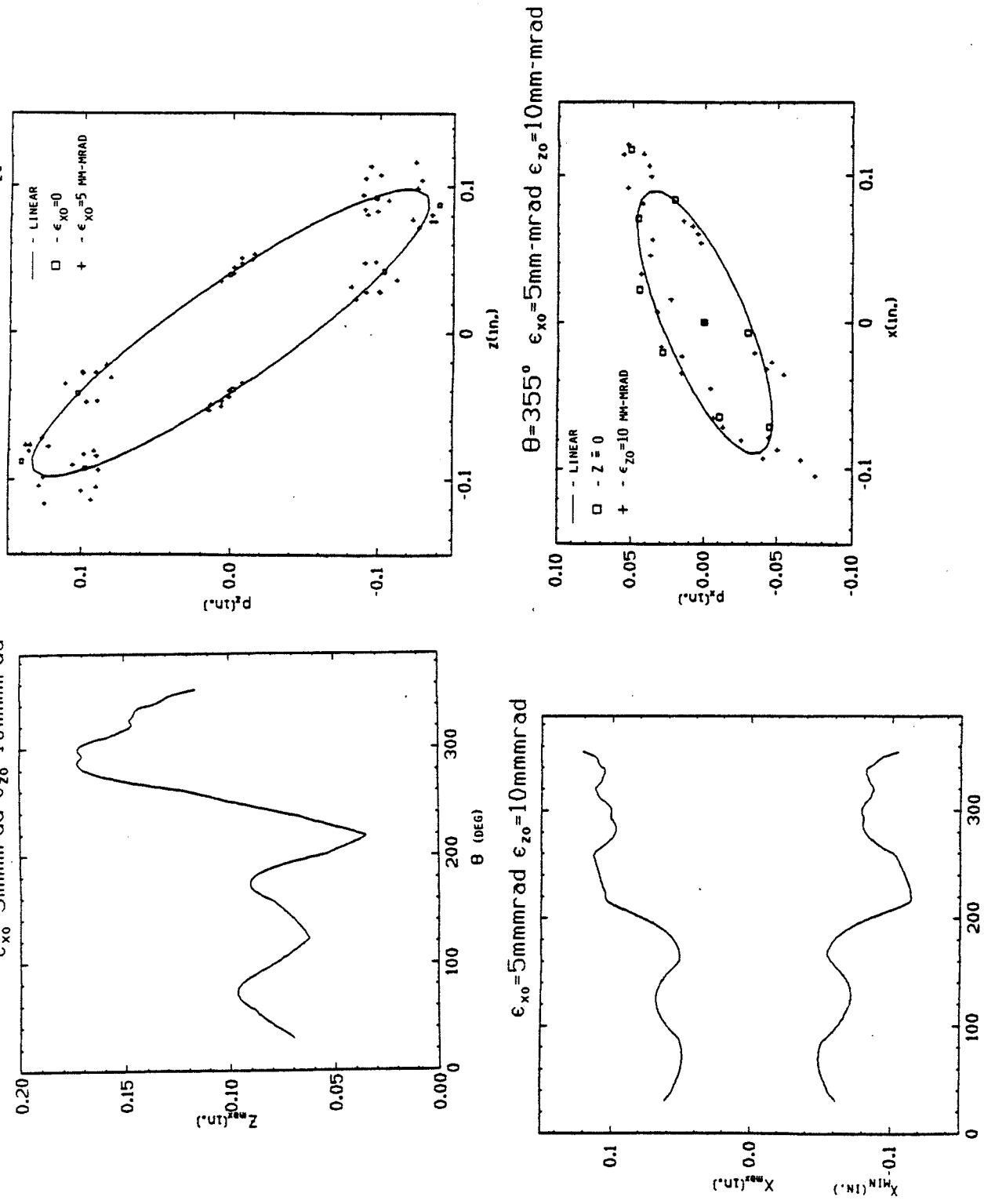

FIG. 17.--A study of extraction orbits in the 1203 field with off median plane components of the focusing bar field computed exactly and with the main field computed to fourth order. The graphs on the left show axial and radial envelopes. Graphs on the right show the phase space distribution in z and in r at the field edge. For comparison the ellipses in the two right hand figures are computed with linearized equations and fields.

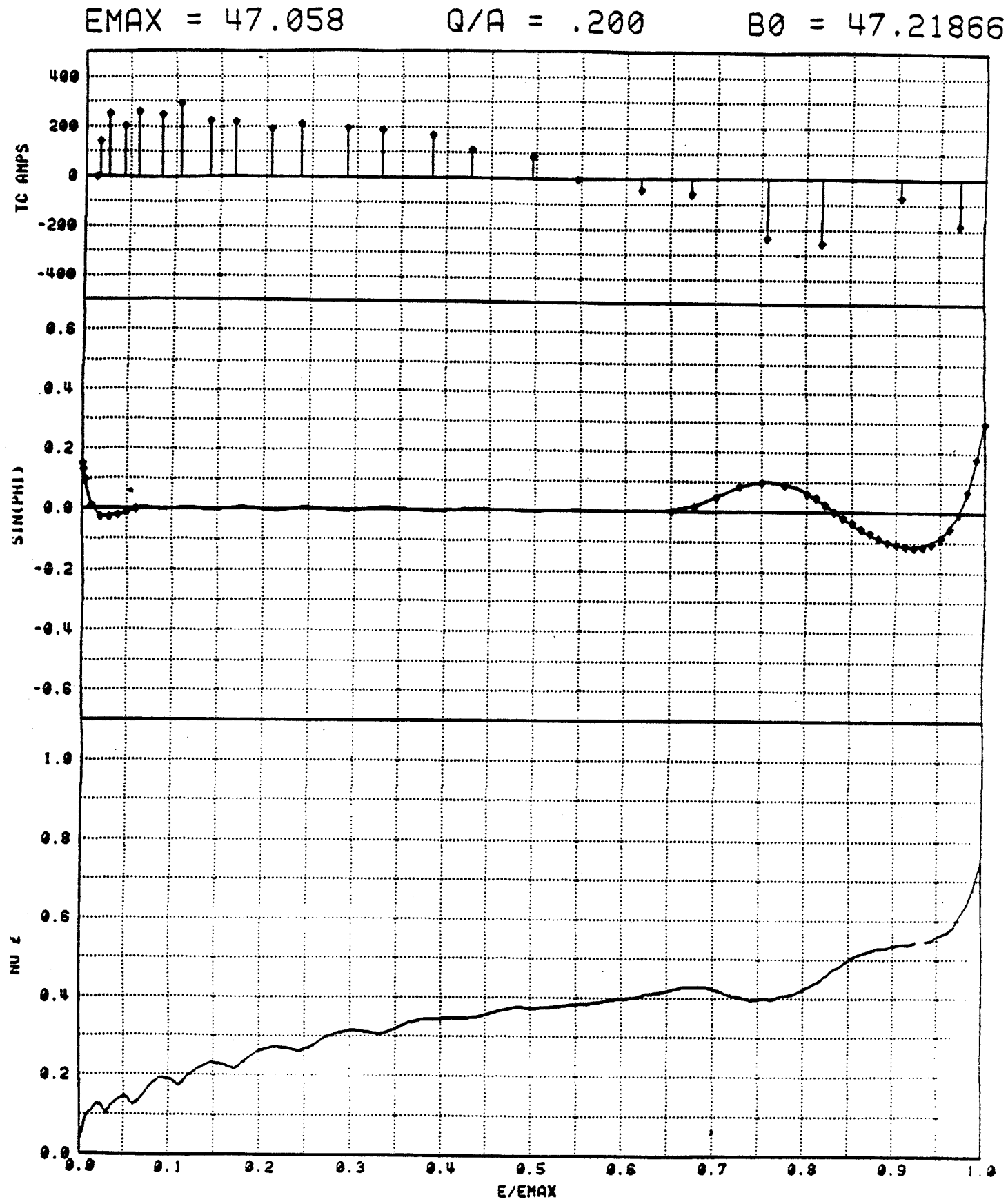

FIG. 18.--Results from the trim coil fitting code for the base magnetic field. The starting point of a self-consistent extraction design calculation.

DEF	TH BAR	R BAR	AL BAR	R RAY	AL RAY	X AV
7	54.50	40.335	-1.600	40.365	-1.580	0.003
9	214.50	41.995	0.000	42.025	0.176	0.004
10	259.50	42.733	1.900	42.751	2.287	-0.002
11	293.00	43.998	3.400	44.014	3.450	0.002
12	312.80	45.080	5.300	45.100	5.281	0.001
13	321.00	45.827	6.900	45.847	6.935	0.002
14	331.00	46.980	9.300	46.996	9.501	0.001
15	343.00	49.110	14.900	49.122	14.915	0.007

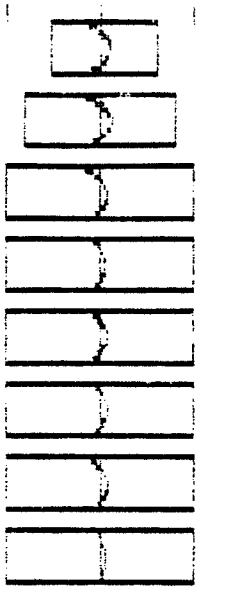

OFF FIELD AT TH = 9.0 350.0 DEG DP = 0.1916 ,DPR/P = 0.0005

R = 39.8900 PR = 2.1300 E = 47.10

DEF	TH1	TH2	TYP	E,B,R	DBR,AL	DE1	DE2
6	31.00	90.00	1	83.500	0.000	0.000	0.000
7	90.84	93.15	3	40.335	-1.600	0.000	0.000
8	151.00	210.00	1	83.500	0.000	0.000	0.000
9	211.00	218.00	3	41.995	0.000	0.000	0.000
10	254.48	262.51	3	42.733	1.900	0.000	0.000
11	290.49	295.50	3	43.998	3.400	0.000	0.000
12	308.99	314.98	3	45.080	5.300	0.000	0.000
13	318.00	323.96	3	45.827	6.900	0.000	0.000
14	328.02	333.98	3	46.980	9.300	0.000	0.000
15	340.07	345.86	3	49.110	14.900	0.000	0.000
16	210.86	218.15	4	40.335	-1.600	0.000	0.000
17	330.86	338.15	4	40.335	-1.600	0.000	0.000
18	91.00	98.00	4	41.995	0.000	0.000	0.000
19	331.00	338.00	4	41.995	0.000	0.000	0.000
20	93.08	96.92	4	42.950	0.000	0.000	0.000
21	151.13	154.87	4	44.000	0.000	0.000	0.000

FIG. 19.--The first trial extraction orbit calculated with electric deflectors which are assumed to be centered on the orbit, and with focusing bar clusters positioned as shown in the tabular data. The graphs at the upper right show the curvature of the ray relative to the assumed straight line bar elements.

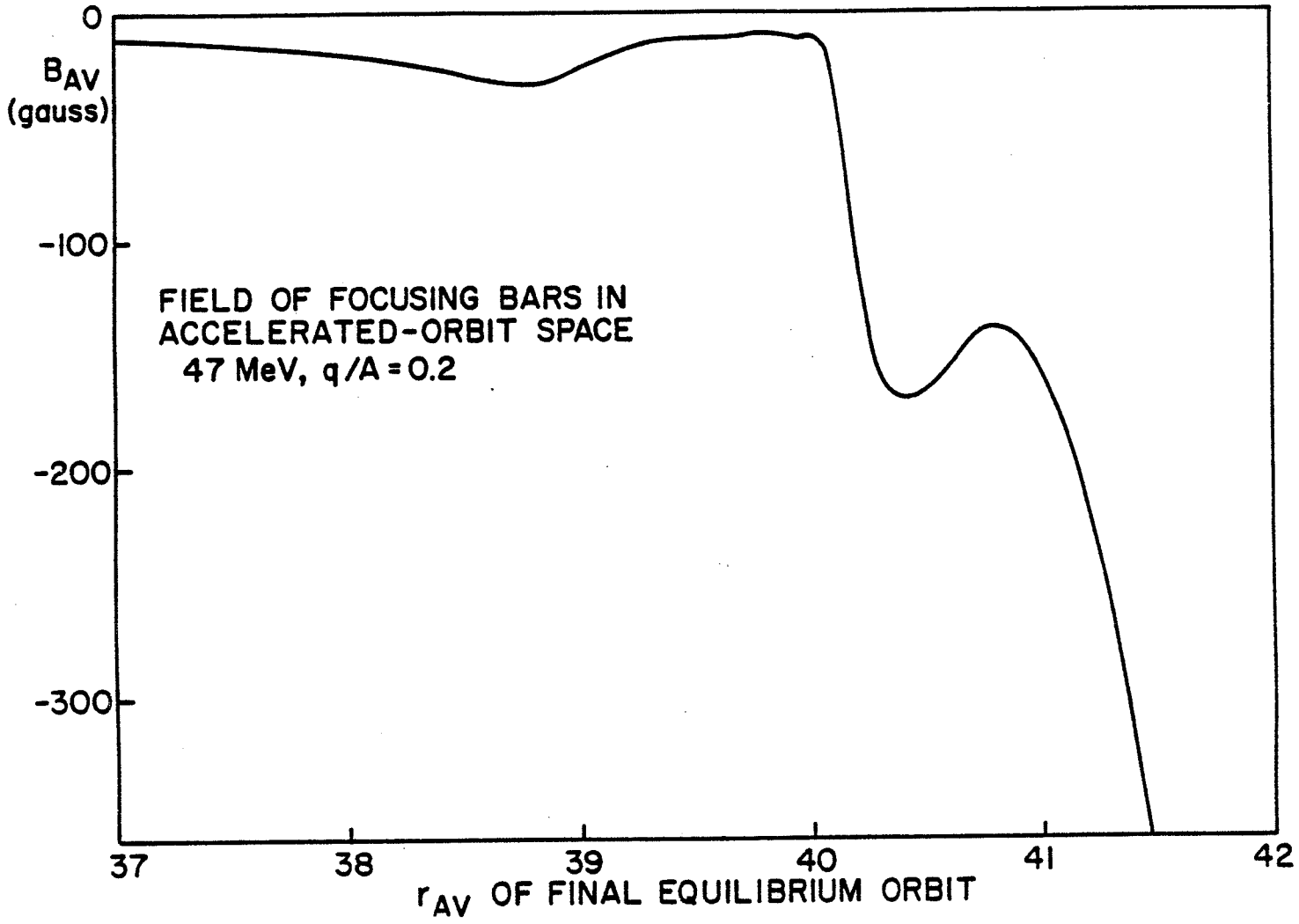

FIG. 20.--Computation of the change in the azimuthal average of the magnetic field in the internal beam space due to the focusing bars of Figure 19.

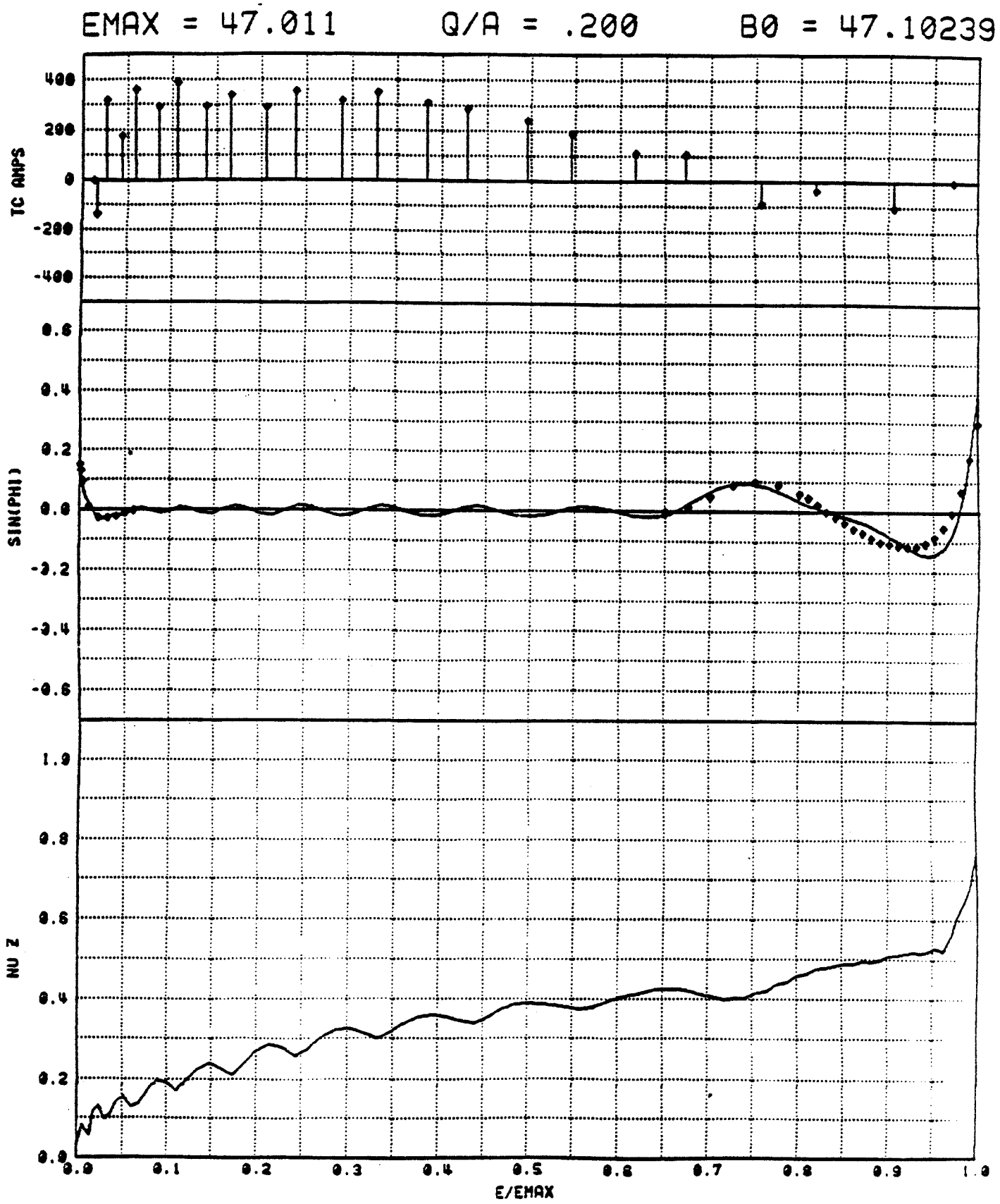

FIG. 21.--Repeat of the trim coil fitting of Figure 18, but with the magnetic field of the bar array included (from Figure 19).

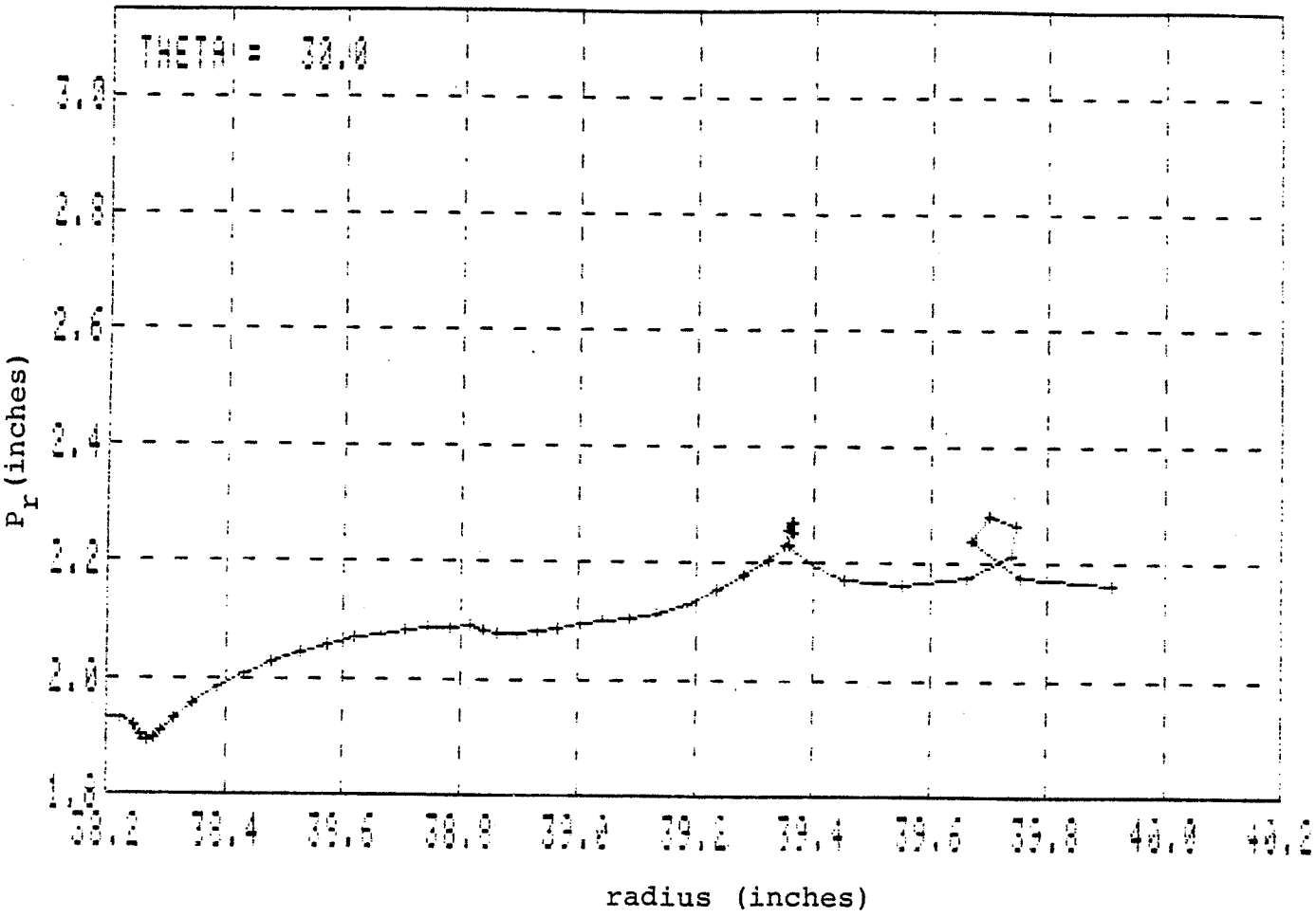

FIG. 22.--Phase space plot of an orbit accelerated backward from the extraction orbit initial condition with a search on the variable extraction field bump (produced by unbalancing the currents in the outer trim coils) to connect this orbit on to a well centered internal orbit. The bunching of turns at the lower left indicates that the orbit is not completely centered at this stage -- further improvement of the centering is not worthwhile at this stage, however, since the extraction elements have not yet been cycled into their final position.

DEF	TH BAR	R BAR	AL BAR	R RAY	AL RAY	X AV
7	64.50	40.375	-1.500	40.409	-1.513	0.006
9	214.50	42.050	0.000	42.063	0.224	0.009
10	259.50	42.794	1.900	42.812	2.160	-0.002
11	293.00	44.033	3.400	44.049	3.294	0.002
12	312.00	45.102	5.200	45.122	5.148	0.002
13	321.00	45.842	6.900	45.863	6.782	0.004
14	331.00	46.988	9.300	47.005	9.456	0.002
15	343.00	49.115	14.900	49.122	14.875	-0.001

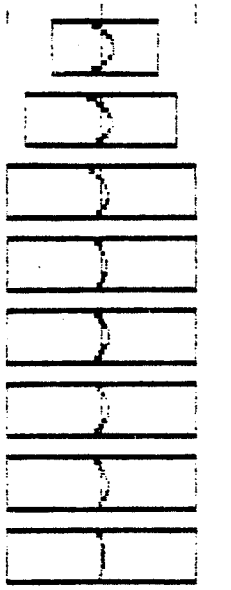

OFF FIELD AT TH = 0.0 350.0 DEG DR = 0.1885 , DPR/P = 0.0002

R = 39.9100 PR = 2.1650 E = 47.00

DEF	TH1	TH2	TYP	E,B,R	DBR,AL	DE1	DE2
6	21.00	90.00	1	85.500	0.000	0.000	0.000
7	90.87	98.15	3	40.375	-1.500	0.000	0.000
8	151.00	210.00	1	85.500	0.000	0.000	0.000
9	211.00	218.00	3	42.050	0.000	0.000	0.000
10	256.49	262.50	3	42.794	1.900	0.000	0.000
11	290.49	295.50	3	44.033	3.400	0.000	0.000
12	308.99	314.98	3	45.102	5.200	0.000	0.000
13	318.01	323.96	3	45.842	6.900	0.000	0.000
14	328.02	333.98	3	46.988	9.300	0.000	0.000
15	340.07	345.86	3	49.115	14.900	0.000	0.000
16	210.87	218.15	4	40.375	-1.500	0.000	0.000
17	330.87	338.15	4	40.375	-1.500	0.000	0.000
18	91.00	98.00	4	42.050	0.000	0.000	0.000
19	331.00	338.00	4	42.050	0.000	0.000	0.000
20	93.08	96.92	4	42.950	0.000	0.000	0.000
21	151.13	154.87	4	44.000	0.000	0.000	0.000

FIG. 23.--Repeat of the runs from Figure 19 but using the base magnetic field from the fit of Figure 21. Small changes in bar positions have been made relative to the runs in Figure 19 in order to center the orbit in the bars in the revised field.

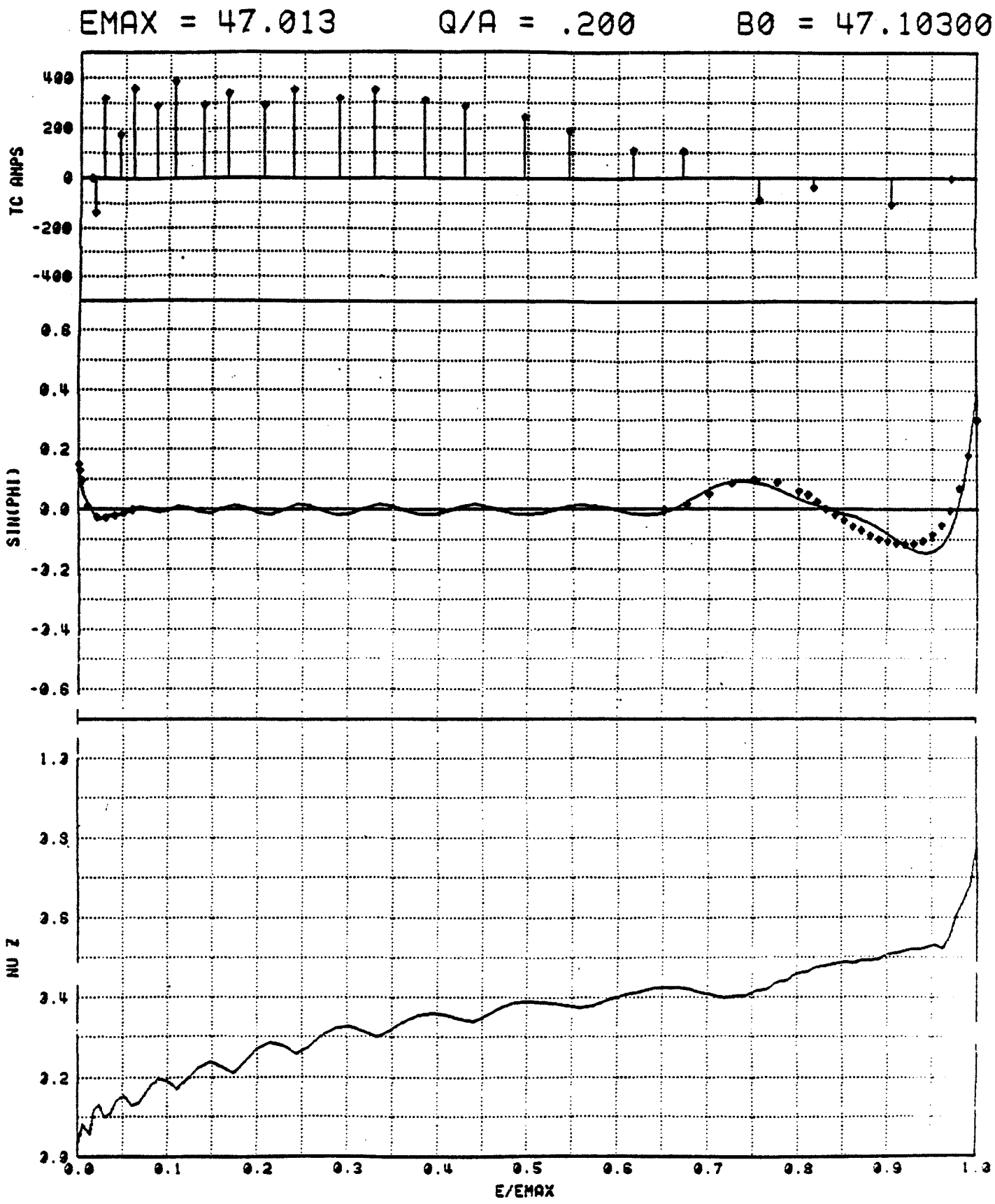

FIG. 24.--Results from a third run of the trim coil field fitting program. This run includes the average field produced by the family of bars at the locations given in Figure 23.

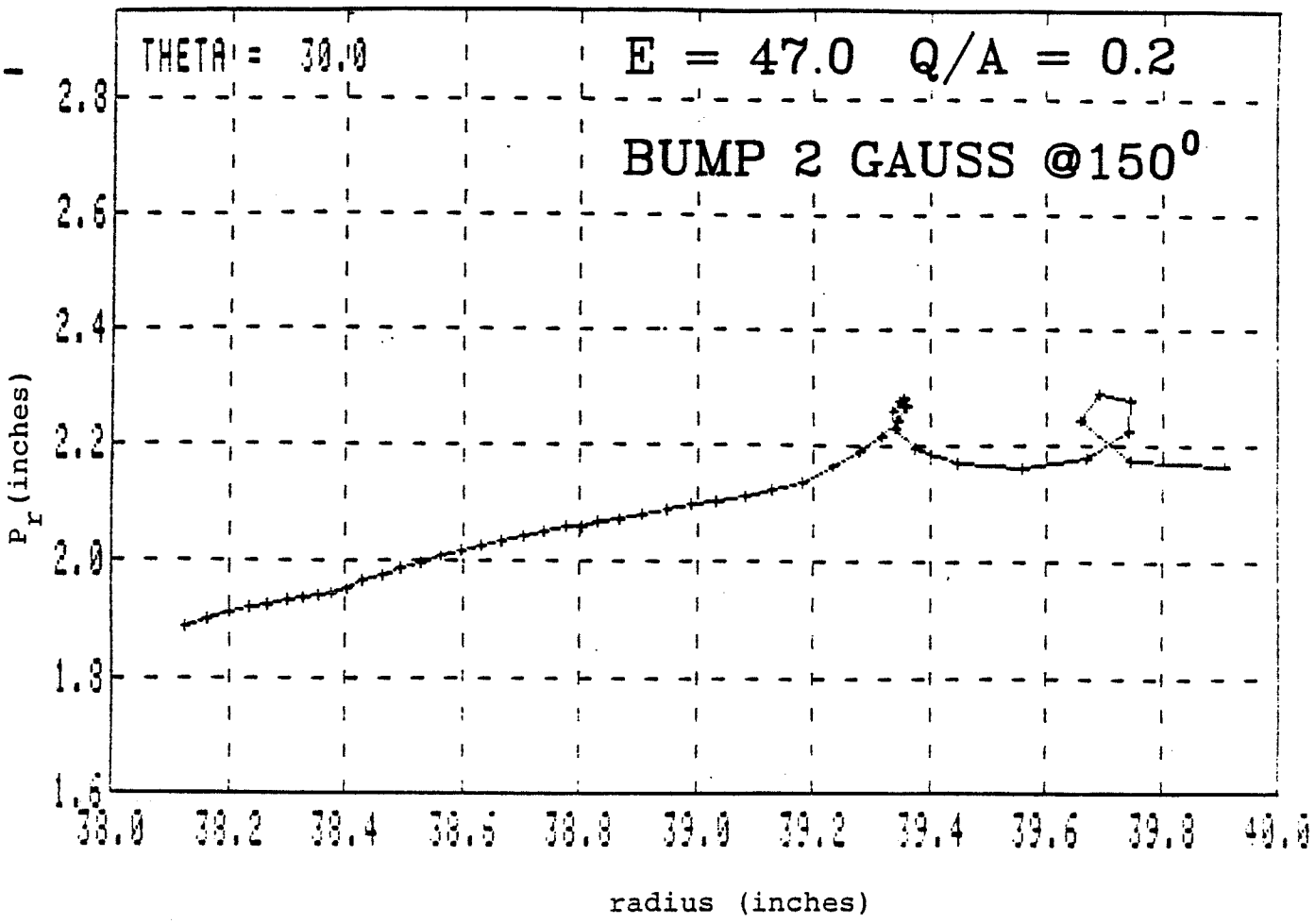

FIG. 25.--Backward run from the Figure 23 initial condition where the extraction field bump has been adjusted to match the extraction orbit to a well centered internal orbit.

DEF	TH BAR	R BAR	AL BAR	R RAY	AL RAY	X AV
7	94.50	40.375	-1.500	40.407	-1.515	0.206
9	214.50	42.050	0.000	42.078	0.220	0.003
10	258.50	42.794	1.900	42.807	2.162	-0.007
11	297.00	44.033	3.400	44.045	3.394	-0.002
12	312.00	45.102	5.200	45.118	5.147	-0.003
13	321.02	45.842	6.900	45.853	6.784	-0.001
14	331.00	46.988	9.300	47.001	9.453	-0.002
15	343.00	49.115	14.900	49.119	14.878	-0.005

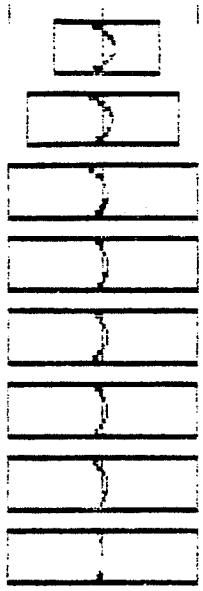

OFF FIELD AT TH = 0.0 750.0 DEG DR = 0.1852 ,DP/P = 0.0002

R = 39.9100 PR = 2.1450 E = 47.00

DEF	TH1	TH2	TYP	E,B,R	DSR,AL	DE1	DE2
6	31.00	90.00	1	85.500	0.000	0.000	0.000
7	90.87	98.15	3	40.375	-1.500	0.000	0.000
8	151.00	210.00	1	85.500	0.000	0.000	0.000
9	211.00	218.00	3	42.050	0.000	0.000	0.000
10	256.49	262.50	3	42.794	1.900	0.000	0.000
11	290.49	295.50	3	44.033	3.400	0.000	0.000
12	303.99	314.98	3	45.102	5.200	0.000	0.000
13	318.01	323.96	3	45.842	6.900	0.000	0.000
14	328.02	333.93	3	46.988	9.300	0.000	0.000
15	340.07	345.86	3	49.115	14.900	0.000	0.000
16	210.87	218.15	4	40.375	-1.500	0.000	0.000
17	330.87	338.15	4	40.375	-1.500	0.000	0.000
18	91.00	98.00	4	42.050	0.000	0.000	0.000
19	331.00	338.00	4	42.050	0.000	0.000	0.000
20	93.08	96.92	4	42.950	0.000	0.000	0.000
21	151.13	154.87	4	44.000	0.000	0.000	0.000

FIG. 26.--Tracking of the central ray through the extraction elements with the main field as defined in Figure 24. The orbit is adequately centered in the extraction elements without changing their position, i.e. the field used for this orbit is that of exactly the same magnet as the field used in Figure 24, so that the calculation is now "self-consistent".

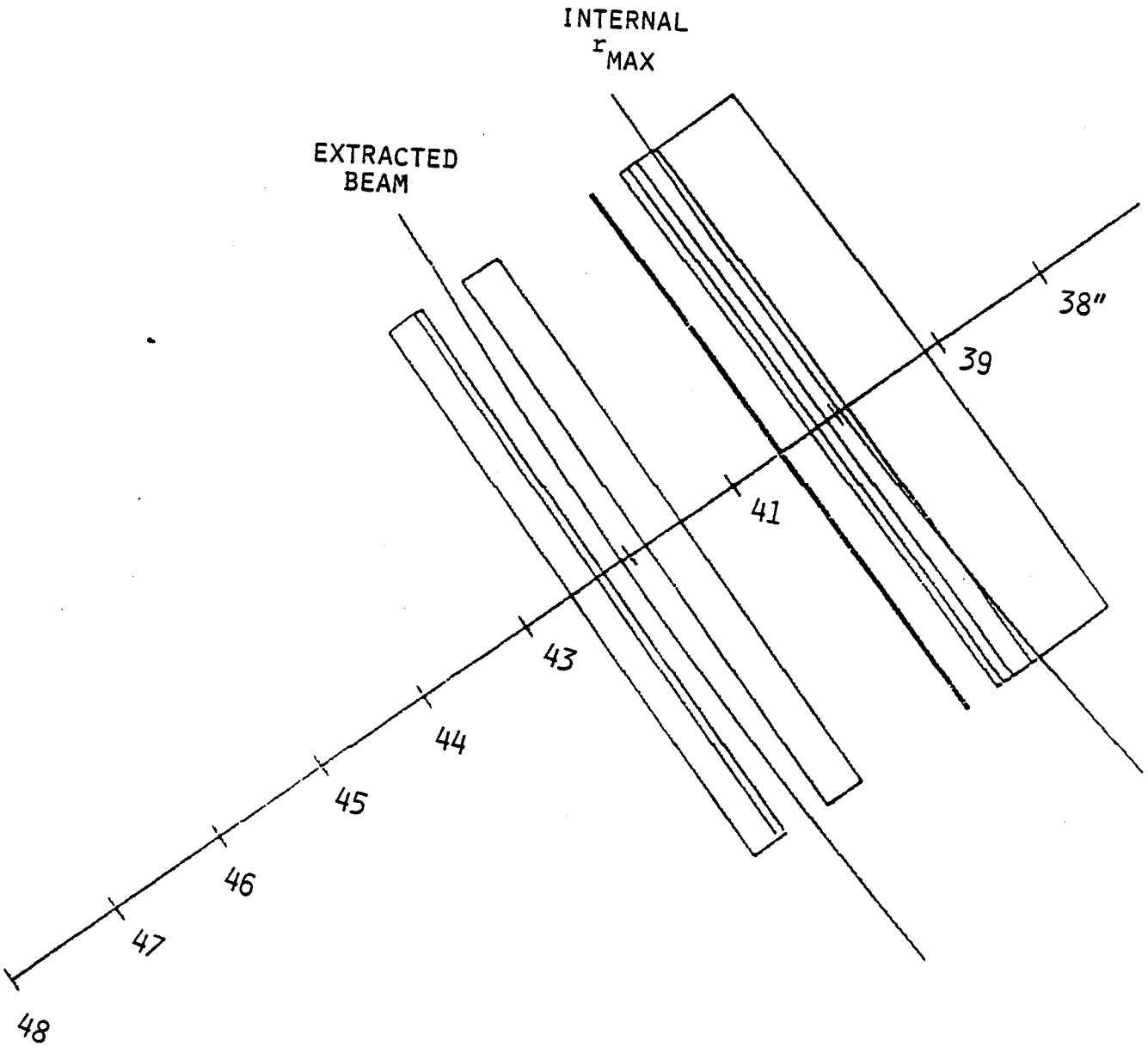

FIG. 27.--Large scale radial plot of the maximum radius internal ray and the extracted beam central ray in the vicinity of the θ=214.5° extraction elements. Noting from Figures 3 and 4 the location of the magnetic elements penetrating the median plane, adequate clearances are seen to exist.

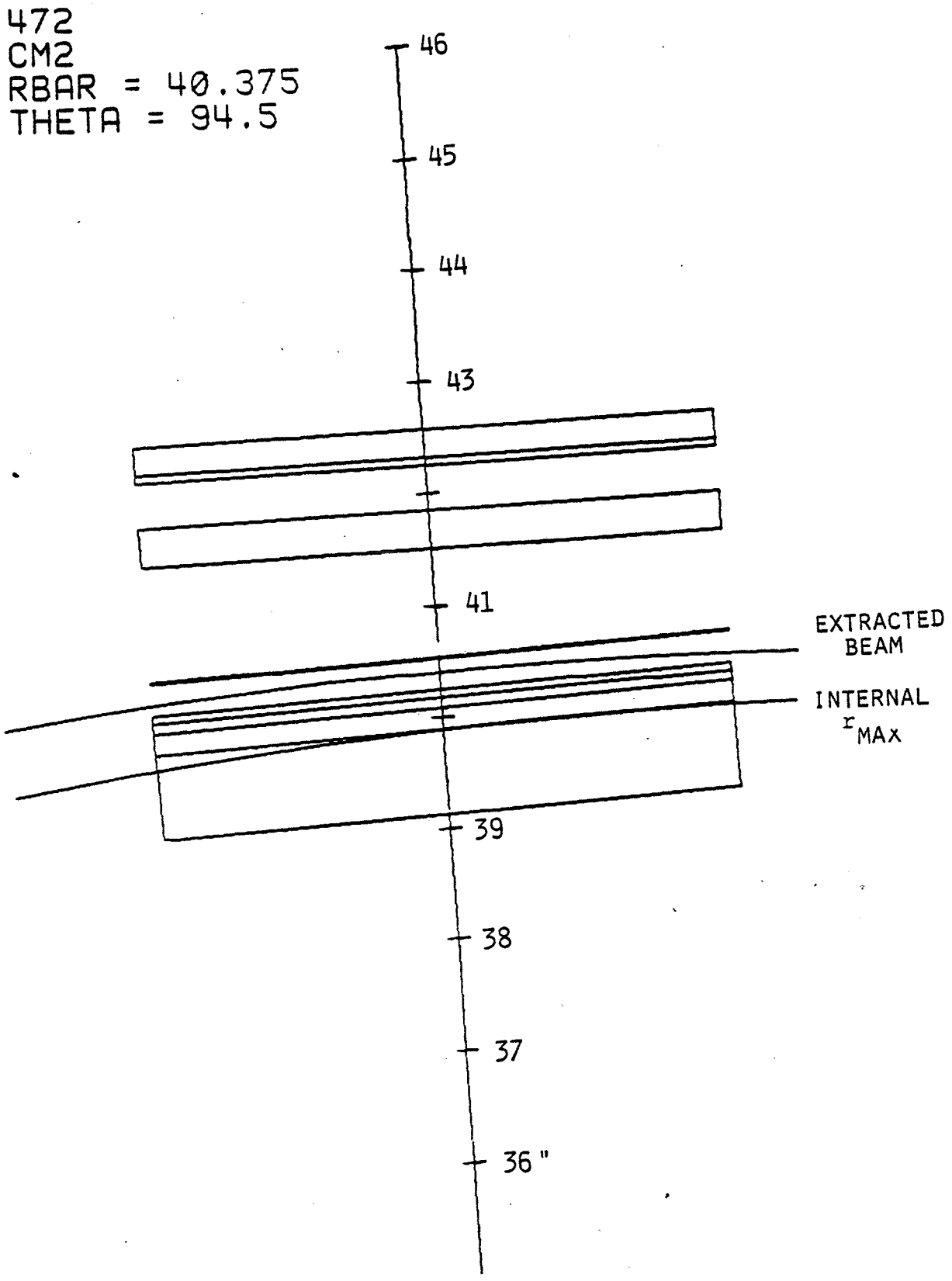

FIG. 28.--Graph of the same form as Figure 27 but at θ=94.5. Clearances at this azimuthal location are also acceptable.

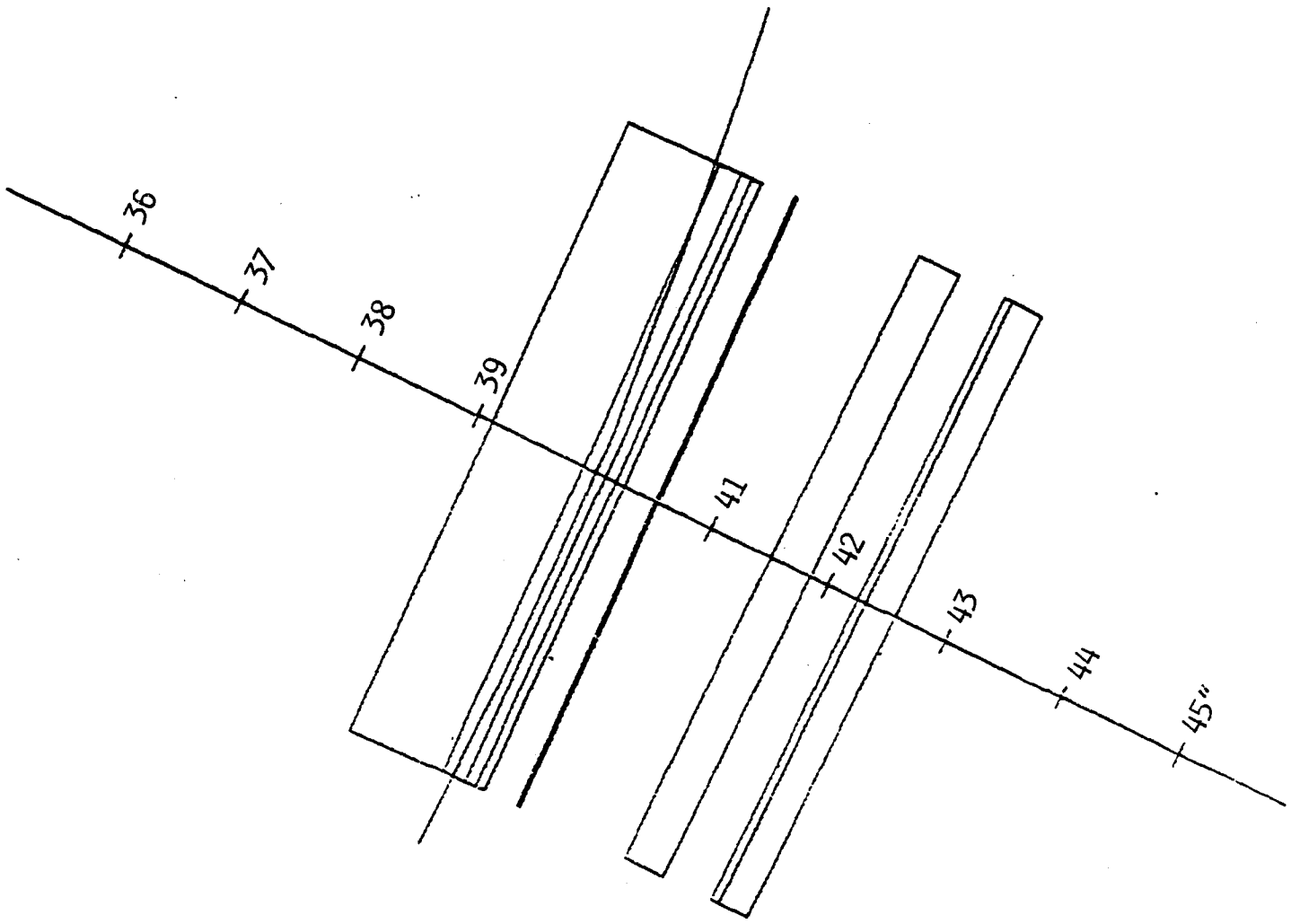

FIG. 29.--Graph of the same form as Figure 27 but at θ=334.5. Clearances at this azimuthal location are also acceptable.